

Improvements on perturbative oscillation formulas including non-standard neutrino Interactions

M. E. Chaves,^{a,b,c} D. R. Gratieri,^d O. L. G. Peres^{c,1}

^a*Instituto de Física - UFF, 24210-310, Niterói RJ, Brazil*

^b*Instituto de Ciências Exatas - UFF, 27213-145, Volta Redonda RJ, Brazil*

^c*Instituto de Física Gleb Wataghin - UNICAMP, 13083-859, Campinas SP, Brazil*

^d*Escola de Engenharia Industrial Metalúrgica de Volta Redonda - UFF, 27225-125, Volta Redonda RJ, Brazil*

E-mail: mchaves@ifi.unicamp.br, [ORCID:0000-0001-7396-081X](https://orcid.org/0000-0001-7396-081X),
drgratieri@id.uff.br, [ORCID:0000-0002-4561-5805](https://orcid.org/0000-0002-4561-5805),
orlando@ifi.unicamp.br, [ORCID:0000-0003-2104-8460](https://orcid.org/0000-0003-2104-8460)

ABSTRACT: We use perturbation theory to obtain neutrino oscillation probabilities, including the standard mass-mixing paradigm and non-standard neutrino interactions (NSI). The perturbation made in standard parameters $\Delta m_{21}^2/\Delta m_{31}^2$ and $\sin^2(\theta_{13})$ and in the non-diagonal NSI parameters, but keep diagonal NSI parameters non-perturbated. We perform the calculation for the channels $\nu_\mu \rightarrow \nu_e$ and $\nu_\mu \rightarrow \nu_\mu$. The resulting oscillation formulas are compact and present functional structure similar to the standard oscillation (SO) case. They apply to a wide range in the allowed NSI space of parameters and include the previous results from perturbative approaches as limit cases. We also take advantage of have compact formulas to *explain* the origin of the degeneracies in the neutrino probabilities in terms of the invariance of amplitude and phase of oscillations. Then we determine analytically the multiple sets of combinations of SO and NSI parameters that result in oscillation probabilities identical to the SO case.

¹Corresponding author.

Contents

1	Introduction	1
2	Perturbative approaches and the neutrino time-evolution	6
3	Perturbation Theory with NSI	6
4	Results for perturbation theory until second order in expansion parameter, κ^2	11
5	Study of degeneracies in the neutrino probability	14
5.1	Degenerescence type 2, only NSI parameters	17
5.2	Degenerescence type 3, standard oscillation mixing parameters and NSI parameters	19
5.2.1	Degenerescence type 3, assuming different mixing angles	22
6	Conclusions	24
A	Explicit relation between NSI parameters in flavor basis and propagation basis	33
B	Formalism to perturbation theory for neutrino oscillations	33
C	Muon neutrino survival probability	34
D	The Non-Standard Interaction Degeneracy	35

1 Introduction

The neutrino mass-mixing formalism that emerged from the last decades of neutrino phenomenology [1–14] is actually known as *Standard Neutrino Oscillations* (SO), and contains 6 different parameters. Two mass differences ($\Delta m_{31}^2, \Delta m_{21}^2$), one CP phase (δ_{CP}) and three mixing angles, ($\theta_{12}, \theta_{13}, \theta_{23}$). The current values for these parameters can be found in the Ref. [15]. As a consequence of SO, the difference between the squared neutrino mass eigenvalues must be $\Delta m_{3l}^2 \approx 2.523 \times 10^{-3} \text{ eV}^2$ and $\Delta m_{21}^2 = 7.39 \times 10^{-5} \text{ eV}^2$, where l mean lighter neutrinos. However, in the *Standard Model of Particles and Fields* (SM) from the Refs. [16–18] and others, neutrinos are included as massless particles. This suggests that the mechanism responsible to give mass to the neutrino should be other than the Brout-Englert-Higgs model [19–21] and the experimental discovery in Refs. [22, 23]. Henceforth, it is straightforward to search for physics beyond the SM to account for neutrino masses. In

this sense, in this work we take into account the so-called *Non-Standard Neutrino Interactions* (NSI) which was firstly proposed by Wolfenstein [24, 25]. NSI can give strong resonant effects even for unmixed neutrinos [26–29] and also for massless neutrinos [29]. In the standard three-neutrino formalism, the time evolution of a neutrino flavor state $\{|\nu_e, \nu_\mu, \nu_\tau\rangle\}$ is given by a Schrodinger-like equation. When NSI are taken into account [30–33], the neutrino time evolution equation assumes the form:

$$i \frac{d}{dt} \begin{pmatrix} \nu_e \\ \nu_\mu \\ \nu_\tau \end{pmatrix} = H \begin{pmatrix} \nu_e \\ \nu_\mu \\ \nu_\tau \end{pmatrix} = (\mathcal{H} + H_{\text{NSI}}) \begin{pmatrix} \nu_e \\ \nu_\mu \\ \nu_\tau \end{pmatrix}, \quad (1.1)$$

where

$$\mathcal{H} = \Delta_{31} \left[U \begin{pmatrix} 0 & 0 & 0 \\ 0 & r_\Delta & 0 \\ 0 & 0 & 1 \end{pmatrix} U^\dagger + r_A \begin{pmatrix} 1 & 0 & 0 \\ 0 & 0 & 0 \\ 0 & 0 & 0 \end{pmatrix} \right], \quad (1.2)$$

and the NSI Hamiltonian, with the complex non-diagonal NSI parameters, and the real diagonal NSI parameters,

$$H_{\text{NSI}} = \Delta_{31} r_A \epsilon' = \Delta_{31} r_A \begin{pmatrix} \epsilon'_{ee} & \epsilon'_{e\mu} & \epsilon'_{e\tau} \\ \epsilon'_{\mu e} & \epsilon'_{\mu\mu} & \epsilon'_{\mu\tau} \\ \epsilon'_{\tau e} & \epsilon'_{\tau\mu} & \epsilon'_{\tau\tau} \end{pmatrix}. \quad (1.3)$$

We adopt the parametrization for the mixing matrix, $U = R(\theta_{23})\tilde{R}(\theta_{13}, \delta_{\text{CP}})R(\theta_{12})$ [34]. Here $R(\theta_{ij})$ is a rotation of the angle θ_{ij} in the i - j plane and $\tilde{R}(\theta_{13}, \delta_{\text{CP}})$ is a complex rotation by an angle θ_{13} and phase δ_{CP} . To keep the notation short, we define,

$$\Delta_{31} = \Delta m_{31}^2 / 2E_\nu, \quad r_\Delta = \frac{\Delta m_{21}^2}{\Delta m_{31}^2}, \quad r_A = \frac{A}{\Delta m_{31}^2}, \quad (1.4)$$

where $\Delta m_{ji}^2 \equiv m_j^2 - m_i^2$ is the mass square difference between the two mass eigenstates j and i . Also, $A = 2E_\nu V_{\text{CC}}$ and $V_{\text{CC}} = \sqrt{2}G_{\text{F}}n_e$ is the matter potential that neutrinos feel while they cross a medium with the electron number density $n_e = N_A \rho \langle Z/A \rangle$. N_A is the number of Avogadro, ρ is the matter density, and $\langle Z/A \rangle$ is the averaged ratio between the nuclear charge and mass number in the medium that neutrino crosses. In this work we assume the following values for the mixing angles, $\sin^2 \theta_{12} = 0.31$, $\sin^2 \theta_{13} = 0.023$, $\sin^2 \theta_{23} = 0.5$, and squared mass differences, $\Delta m_{31}^2 = 2.4 \times 10^{-3} \text{ eV}^2$, $\Delta m_{21}^2 = 7.5 \times 10^{-5} \text{ eV}^2$. In the last term in Eq. (1.1) we include the effective NSI parameters, $\epsilon'_{\alpha\beta}$, as effective matter potentials summed up in medium element in the neutrino time evolution Hamiltonian and which are related to the complex coupling constants $\epsilon_{\alpha\beta}^{\text{fV}}$ by,

$$\epsilon'_{\alpha\beta} = \sum_{\text{f=e,u,d}} Y_f(x) \epsilon_{\alpha\beta}^{\text{fV}}, \quad \alpha, \beta = e, \mu, \tau. \quad (1.5)$$

Here, $Y_f(x) = n_f(x)/n_e(x)$, where $n_f(x)$ is the number of fermions in the medium and the vector coupling $\epsilon_{\alpha\beta}^{\text{fV}} = \epsilon_{\alpha\beta}^{\text{fL}} + \epsilon_{\alpha\beta}^{\text{fR}}$ are the complex coupling parameters in the non-standard

interaction effective Lagrangian

$$-\mathcal{L}_{\text{NSI}}^{\text{eff}} = \sum_{f=e,u,d} \sum_{X=L,R} \epsilon_{\alpha\beta}^{\text{fP}} 2\sqrt{2}G_F (\bar{\nu}_\alpha \gamma_\rho L \nu_\beta) (\bar{f} \gamma^\rho X f) + (c.c), \quad (1.6)$$

where $X = (L, R) = (1 - \gamma^5, 1 + \gamma^5)/\sqrt{2}$. At the fundamental level, $\epsilon_{\alpha\beta}^{\text{fP}} \equiv \frac{G_X}{G_f}$ is related with to couplings of neutrino flavor states with the electrons and quarks due the exchanged boson X and it expresses the ratio between the strength of new interaction, G_X , to the strength of SM weak coupling, G_f .

For the oscillation phenomenology, we can always remove a global phase, which we performed by subtracting a multiple of identity matrix in Eq. (1.1). We choose to subtract $\epsilon'_{\mu\mu} \times$ -Identity matrix and in this way, the only physical parameters for oscillation it will be $\epsilon'_{\tau\tau} - \epsilon'_{\mu\mu}$ and $\epsilon'_{ee} - \epsilon'_{\mu\mu}$. We will redefine the complex matrix ϵ' in terms of the complex matrix ϵ ,

$$\epsilon' \rightarrow \epsilon \equiv \Delta_{31} r_A \begin{pmatrix} \epsilon_{ee} & \epsilon_{e\mu} & \epsilon_{e\tau} \\ \epsilon_{\mu e} & \epsilon_{\mu\mu} & \epsilon_{\mu\tau} \\ \epsilon_{\tau e} & \epsilon_{\tau\mu} & \epsilon_{\tau\tau} \end{pmatrix} = \Delta_{31} r_A \begin{pmatrix} \epsilon'_{ee} - \epsilon'_{\mu\mu} & \epsilon'_{e\mu} & \epsilon'_{e\tau} \\ \epsilon'_{\mu e} & 0 & \epsilon'_{\mu\tau} \\ \epsilon'_{\tau e} & \epsilon'_{\tau\mu} & \epsilon'_{\tau\tau} - \epsilon'_{\mu\mu} \end{pmatrix}, \quad (1.7)$$

and we will work for now on, with the variables, $\epsilon_{\alpha\beta}$, that for $\alpha = \beta$ are real parameters and for $\alpha \neq \beta$ are complex parameters.

Since the first studies on NSI [24, 26–29, 35–41], now we have an intense activity on this topic [30, 33, 42–87] and recent reviews can be found in the Refs. [31–33, 52]. For instance, in Ref. [26, 27] it was proposed as a solution for solar neutrino problem and confirmed in Ref. [39]. But from the results of KamLand experiment [7], the only possibility it is a mixed solution of NSI and mass-mixing as discussed in Ref. [88]. Similarly for atmospheric neutrinos, the NSI scenario was able to explain the muon neutrino deficit at lower energy as discussed in Ref. [38] but not the muon neutrino deficit at higher energies in such way that nowadays only mixed solutions are possible. Bounds on the NSI parameters were made in the literature under two assumptions,

1. assume one and only one non-zero NSI parameter [30, 60, 80, 81]
2. assume more than one non-zero NSI parameter [38, 39, 44, 62, 65, 68, 73–77, 79, 82–86, 88–91]

One example of the second case it was found in solar neutrino analysis, where two good solutions were found. One solution is compatible with vanishing NSI parameters and mixing angles compatible with the values mentioned above, that have $\theta_{12} < \pi/4$. The other solution, called LMA-Dark solution, it has solar mixing angle $\theta_{12} > \pi/4$, which is possible for large diagonal real parameters NSI, ϵ_{ee} and $\epsilon_{\mu\mu}/\epsilon_{\tau\tau}$ [89]. Another example is the analysis of atmospheric data made in the Ref. [90] where solutions with a large NSI parameter ϵ_{ee} , $\epsilon_{\tau\tau}$, and the magnitude of $\epsilon_{e\tau}$ are virtually identical to the vacuum oscillation and are called *vacuum mimicking* solutions. These two examples are a subset of fundamental degeneracy of neutrino probability, where you can have the same oscillation probability with completely different set of parameters for the mixing parameters and for

the NSI parameters. This fundamental degeneracy happens in neutrino evolution system, Eq. (1.1), called *generalized mass ordering degeneracy* [44]¹,

$$\begin{aligned}
\Delta m_{31}^2 &\rightarrow -\Delta m_{32}^2, \\
\theta_{12} &\rightarrow \pi/2 - \theta_{12}, \\
\delta_{\text{CP}} &\rightarrow 2\pi - \delta_{\text{CP}}, \\
\epsilon_{\alpha\alpha} &\rightarrow -2\delta_{\alpha e} - \epsilon_{\alpha\alpha}, \\
\epsilon_{\alpha\beta} &\rightarrow -\epsilon_{\alpha\beta}^*, \alpha, \beta \neq e, \\
\epsilon_{e\alpha} &\rightarrow \epsilon_{e\alpha}^*.
\end{aligned} \tag{1.8}$$

This degeneracy is exact for neutrinos crossing a constant density medium, as it is in the present long-baseline experiments, which are sensitive to the neutrino oscillation probabilities resulting from the solution of the neutrino evolution described in Eqs. (1.1-1.3). To break this degeneracy, we can use the fact that the differential cross-section for coherent elastic scattering of a ν_α with energy E_ν and a nucleus N with Z protons, N neutrons, and mass M is given by, assuming that the complex NSI parameters [92]

$$\frac{d\sigma_{\nu_\alpha\text{-N}}(E_\nu, T)}{dT} = \frac{G_F^2 M}{\pi} \left(1 - \frac{MT}{2E_\nu^2}\right) Q_\alpha^2, \tag{1.9}$$

where T is the nuclear recoil kinetic energy and

$$\begin{aligned}
Q_\alpha^2 = & \left[(g_V^p + 2\epsilon_{\alpha\alpha}^{uV} + \epsilon_{\alpha\alpha}^{dV}) Z F_Z(|\vec{q}|^2) + (g_V^n + \epsilon_{\alpha\alpha}^{uV} + 2\epsilon_{\alpha\alpha}^{dV}) N F_N(|\vec{q}|^2) \right]^2 \\
& + \sum_{\beta \neq \alpha} \left| (2\epsilon_{\alpha\beta}^{uV} + \epsilon_{\alpha\beta}^{dV}) Z F_Z(|\vec{q}|^2) + (\epsilon_{\alpha\beta}^{uV} + 2\epsilon_{\alpha\beta}^{dV}) N F_N(|\vec{q}|^2) \right|^2,
\end{aligned} \tag{1.10}$$

with

$$g_V^p = \frac{1}{2} - 2\sin^2\theta_W, \quad g_V^n = -\frac{1}{2}. \tag{1.11}$$

Here θ_W is the weak mixing angle, given by $\sin^2\theta_W = 0.23857 \pm 0.00005$ at low energies [93], $F_Z(|\vec{q}|^2)$ and $F_N(|\vec{q}|^2)$ are, respectively, the form factors of the proton and neutron distributions in the nucleus, that depend on the three-momentum transfer $|\vec{q}| \simeq \sqrt{2MT}$.

Recently the first measurement of coherent neutrino-nucleon scattering experiment was made by the COHERENT experiment [94]. Also, there are upper limits for these cross-sections from the CONNIE experiment [95, 96] that it got until now the best limits for light vector mediator search [96]. The coherent neutrino-nucleon scattering measurement allows us to get an independent bound on NSI parameters [61, 94, 97–105]. Using data from the COHERENT experiment [94] we can put bounds on $\epsilon_{\alpha\beta}^{uV}$ and $\epsilon_{\alpha\beta}^{dV}$ for $\alpha = e, \mu$ and $\beta = e, \mu, \tau$.

Furthermore, there is a global analysis of all neutrino oscillation data under the NSI framework [91] that also combine it with this recent results from COHERENT experiment.

¹A note of caution that in Ref. [44] the fundamental degeneracy of the oscillation probability it was formulated using a different convention for mixing matrix that it was not equal to more common used convention in Particle Data definition for mixing matrix [34]. Our Eq. (1.8) it is for Particle Data Group convention.

Indeed, in this analysis, the authors assume all NSI parameters are real, and also subtract a diagonal element $\epsilon_{\mu\mu}$, as we did in Eq. (1.7), which implies that their bounds applies to the parameters $\epsilon_{\alpha\beta}$. The combination of global analysis of neutrino oscillation data and the data from the COHERENT experiment gives upper bounds on the NSI couplings as follows,

$$\epsilon_{\alpha\beta}(\min : \max) \leq \begin{pmatrix} -0.65 : 1.4 & -0.19 : 0.16 & -1.1 : 0.43 \\ -0.19 : 0.16 & -- & -0.05 : 0.04 \\ -1.1 : 0.43 & -0.05 : 0.04 & -0.025 : 0.50 \end{pmatrix}. \quad (1.12)$$

We also acknowledged the table of $\Delta\chi^2 \times$ NSI parameters in Ref. [106].

From these results we can notice a pattern on the bounds on NSI parameters,

1. the diagonal NSI parameters can have larger values $\epsilon_{\alpha\alpha} \sim (-0.65 \rightarrow 1.4)$,
2. non-diagonal NSI parameters can have at maximum $\epsilon_{\alpha\beta} \simeq (-1.1 \rightarrow 0.43)$ for $\alpha \neq \beta$,
3. also for the bounds on the non-diagonal NSI parameters there is a hierarchy. The bound on $\epsilon_{e\tau}$, is relatively weak compared with the bound on $\epsilon_{e\mu}$ and $\epsilon_{\mu\tau}$. From this we assume, that $\epsilon_{e\tau}$ can be larger than $\epsilon_{e\mu}$ and $\epsilon_{\mu\tau}$.

This pattern of the bounds and also the results from Refs. [89, 90] inspire us to think what can be the effects of *significant diagonal NSI elements* in the phenomenology, and it was one of the motivations of this work. Indeed, in the recent analysis of the future experiment's sensitivity to the NSI [44, 62, 68], large diagonal NSI elements are also allowed. In these works it observes two branches for the allowed regions, the first branch (*i*) it is compatible with the scenario of null NSI, and it has as best fit values all NSI parameters $\epsilon_{\alpha\beta} \sim 0$, and second branch (*ii*) it is compatible with a scenario with significant NSI parameters.

The fact that large *diagonal* NSI parameters are still allowed it is not widely known. For a first approach what can make the effects of large diagonal NSI element in the neutrino phenomenology, we decide to study the effects in the neutrino propagation. We choose to use the perturbation theory approach, and we can get an analytical formula for the neutrino probability.

Indeed, after the seminal work from Ref. [107], a plethora of methods to solve the Eq. (1.1) based on perturbative strategies emerged in the literature. For the standard case (without NSI) it is used that some parameters of neutrino time evolution Hamiltonian are today known to be small, $\sin^2(\theta_{13}) \approx \Delta m_{21}^2 / \Delta m_{31}^2 \approx 0.03$. See for example [30, 65, 73–77, 80–82, 84–86, 107–109]. For NSI, also there is the use of the perturbation theory, but due it is still unknown the true strength of NSI parameters and we have different assumptions made in the literature [30, 65, 73–77, 80–82, 84–86, 103].

The paper is organized as follows: In Section 2, we introduce the perturbative methods, the formalism of neutrino propagation through the quantum perturbation theory of Hamiltonian systems, without NSI, and in Section 3 with NSI. In Section 4, we present the resulting probabilities from the perturbation method, compare it with numerical solutions,

and apply it to the DUNE case. In Section 5, we show how the results from perturbation theory can explain the degenerate behavior of neutrino time-evolution. Conclusions are in Section 6.

2 Perturbative approaches and the neutrino time-evolution

The NSI formalism, as it is given in Eq. (1.1), describes a three-neutrino system with the addition of NSI parameters. Firstly we will discuss the standard case, where we have only the three-neutrino system with standard matter effect and later the case for NSI. In the standard oscillation case, exact solutions of Eq. (1.1) are possible for vacuum [110] as well as for constant matter case [107, 111, 112]. However, for varying matter potentials, full solutions of the Schroedinger equation are only possible numerically. Henceforth, a common approach in the literature is to use perturbative methods to found approximate semi-analytical solutions. Such works use the perturbative quantum theory for time-dependent Hamiltonian [113]. Even the solution for constant density is not easily known, understandable the physical meaning. A solution is given by Refs. [114, 115]² use the eigenvalues and eigenvectors of the 3×3 matrix that is not much illuminating. Other analytical solutions involve

- a perturbative approach of full oscillation probability such as (I) small θ_{13} perturbative expansion [107] (II) *large* θ_{13} expansion [30, 108].
- a specific rotation that made the problem separable in two 2×2 systems [65, 117],
- diagonalization of neutrino evolution [78].

In Ref. [109], three neutrino oscillation probabilities are developed within the perturbation theory for an arbitrary density profile. Because of the non-zero value of θ_{13} [8, 118], further developments of this formalism were done to extend the theory [30, 108]. Therefore, in this work we adopt the expansion parameters, the variables, $(\sin(\theta_{13}), r_\Delta, \epsilon_{\alpha\beta})$ for $\alpha \neq \beta$. The state of the art of perturbative methods applied to neutrino time evolution was studied in [116, 119]. In a recent analysis in Ref. [71], perturbation theory is used to analytically take into account the different density values that neutrinos feel while crossing the pathway for DUNE experiment [120]. In Section 3 we will show a perturbative approach that has applicability of NSI parameters $\epsilon_{\alpha\beta}$ for larger diagonal NSI elements.

3 Perturbation Theory with NSI

Here we address the formalism to solve neutrino time-evolution, including NSI. We use perturbation theory through Dyson Series and consider as guidelines that the final expression for the probabilities should obey the following conditions:

1. - To agree with the numerical solution;

²We should be aware that there are mistyping in Ref. [114], accordingly with Ref. [116]

2. - Allow us to use the perturbation theory for all the set of values of NSI parameters given in Eq. (1.12);
3. - Be concise enough to allow direct interpretation and use;
4. - Have the functional form as close as possible to the standard oscillation case in the presence of matter effects.

In the case of standard solution for neutrino oscillation (the limit of $\epsilon_{\alpha\beta} \rightarrow 0$ in Eq. (1.1)) we have that the standard matter effect it is invariant under θ_{23} rotation. If we define a propagation basis such as

$$|\tilde{\nu}_\alpha\rangle = [R(\theta_{23})]^\dagger |\nu_\alpha\rangle, \quad (3.1)$$

where $R(\theta_{23})$ is the rotation matrix by the mixing angle θ_{23} as defined previously, then we have two effects:

1. the mixing angle θ_{23} did not appear the new evolution equation for neutrinos in the $|\tilde{\nu}_\alpha\rangle$ basis,
2. the Hamiltonian presents a more simpler format, having a block-diagonal form.

Once we solved the neutrino evolution in the $|\tilde{\nu}_\alpha\rangle$ basis we should rotated back to get the solution of neutrino evolution. This made the perturbative form of the evolution matrix for standard neutrino oscillation to be more simpler to write. When we include the NSI term this invariance under a rotation on θ_{23} it is broken. However, we can keep a simpler format for Hamiltonian, even in the NSI formalism, where the new Hamiltonian is changed to $H \rightarrow \tilde{H}$, where

$$\tilde{H} = [R(\theta_{23})]^\dagger H R(\theta_{23}) = [R(\theta_{23})]^\dagger (\mathcal{H}) R(\theta_{23}) + [R(\theta_{23})]^\dagger (H_{\text{NSI}}) R(\theta_{23}), \quad (3.2)$$

where the last term can be recast in terms of the new NSI parameters $\tilde{\epsilon}$,

$$[R(\theta_{23})]^\dagger (H_{\text{NSI}}) R(\theta_{23}) = \Delta_{31} r_A [R(\theta_{23})]^\dagger \epsilon R(\theta_{23}) \equiv \Delta_{31} r_A \tilde{\epsilon}. \quad (3.3)$$

Here the notation $\tilde{\epsilon}$ will be a shorthand for the product $[R(\theta_{23})]^\dagger \epsilon R(\theta_{23})$. For each non-diagonal element $\tilde{\epsilon}_{\alpha\beta} = |\tilde{\epsilon}_{\alpha\beta}| e^{i\phi_{\alpha\beta}}$ for all $\alpha \neq \beta = e, \mu, \tau$ and the diagonal elements are always real numbers. The explicit relation between ϵ and $\tilde{\epsilon}$ is given in the Appendix A.

A good way to achieve the conditions 1-4 is to create a hierarchy of NSI parameters in the Hamiltonian. We will divide our full Hamiltonian \tilde{H} as given in Eq. (3.2) as follows. We will define a non-perturbated Hamiltonian that we will called $\tilde{H}^{(0)}$

$$\tilde{H}^{(0)} = \Delta_{31} \begin{pmatrix} r_A & 0 & 0 \\ 0 & 0 & 0 \\ 0 & 0 & 1 \end{pmatrix} + \Delta_{31} r_A \begin{pmatrix} \tilde{\epsilon}_{ee} & 0 & 0 \\ 0 & 0 & 0 \\ 0 & 0 & \tilde{\epsilon}_{\tau\tau} \end{pmatrix}. \quad (3.4)$$

In this Hamiltonian, we incorporate the diagonal NSI parameters, $\tilde{\epsilon}_{ee}$ and $\tilde{\epsilon}_{\tau\tau}$ (the other $\tilde{\epsilon}_{\mu\mu}$ was already subtracted off). We will consider this as the non-perturbated Hamiltonian. In

other words, we will made no expansions for the diagonal NSI elements. Here is *one of the choices of this work*, to incorporate the diagonal NSI parameters as the non-perturbative parameters. This it will have impact on the better expansion for larger diagonal NSI elements, but still inside the 3σ allowed values at present from global fits, as it will be clear in Section 4 and in Figure 1.

For the next term, we include it in the first term of perturbation Hamiltonian. We choose to have the s_{13} and we incorporate the NSI parameter $\tilde{\epsilon}_{e\tau}$, as follows

$$\tilde{H}^{(a)} = \Delta_{31} \begin{pmatrix} 0 & 0 & s_{13}e^{-i\delta_{\text{CP}}} \\ 0 & 0 & 0 \\ s_{13}e^{i\delta_{\text{CP}}} & 0 & 0 \end{pmatrix} + \Delta_{31}r_A \begin{pmatrix} 0 & 0 & \tilde{\epsilon}_{e\tau} \\ 0 & 0 & 0 \\ \tilde{\epsilon}_{\tau e} & 0 & 0 \end{pmatrix}. \quad (3.5)$$

With this choice, that it is twofold, we have a block-diagonal format for the perturbed Hamiltonian, and we assume that this NSI parameter is so important as the s_{13} term. Notice that both expansion parameters located in the same entry of the Hamiltonian. The remain NSI parameters *we will choose* to be next-next-order parameter of the perturbation theory, which means that $\tilde{\epsilon}_{e\mu}$ and $\tilde{\epsilon}_{\mu\tau}$ are putting together with the r_Δ parameter. It follows from *our choice* that:

- $\tilde{\epsilon}_{e\mu}$ parameter is assumed to have the same order of magnitude than r_Δ parameter. Also, the parameter enter in the same position of the respective SO term in the Hamiltonian
- Between the available possibilities, *we choose* to assume $\tilde{\epsilon}_{\mu\tau}$ with the same order than r_Δ , since it is not desirable that the parameter appears only at higher orders of the perturbation theory.

$$\tilde{H}^{(b)} = \Delta_{31} \begin{pmatrix} r_\Delta s_{12}^2 + s_{13}^2 & r_\Delta c_{12}s_{12} & 0 \\ r_\Delta c_{12}s_{12} & r_\Delta c_{12}^2 & 0 \\ 0 & 0 & -s_{13}^2 \end{pmatrix} + \Delta_{31}r_A \begin{pmatrix} 0 & \tilde{\epsilon}_{e\mu} & 0 \\ \tilde{\epsilon}_{\mu e} & 0 & \tilde{\epsilon}_{\mu\tau} \\ 0 & \tilde{\epsilon}_{\tau\mu} & 0 \end{pmatrix}, \quad (3.6)$$

Summarizing, the leading expansion parameter is $(\sin\theta_{13}, \tilde{\epsilon}_{e\tau})$ and the next-leading parameters are $r_\Delta, \tilde{\epsilon}_{e\mu}$ and $\tilde{\epsilon}_{\mu\tau}$.

To complete, we should include the remaining parts of full Hamiltonian \tilde{H} that are not include in $\tilde{H}^{(0)}, \tilde{H}^{(a)}$ and $\tilde{H}^{(b)}$, that we split in two Hamiltonian

$$\tilde{H}^{(c)} = -\Delta_{31} \begin{pmatrix} 0 & 0 & (r_\Delta s_{12}^2 + \frac{1}{2}s_{13}^2)s_{13}e^{-i\delta_{\text{CP}}} \\ 0 & 0 & r_\Delta s_{12}c_{12}s_{13}e^{-i\delta_{\text{CP}}} \\ (r_\Delta s_{12}^2 + \frac{1}{2}s_{13}^2)s_{13}e^{i\delta_{\text{CP}}} & r_\Delta s_{12}c_{12}s_{13}e^{i\delta_{\text{CP}}} & 0 \end{pmatrix}, \quad (3.7)$$

and

$$\tilde{H}^{(d)} = -\Delta_{31}r_\Delta \begin{pmatrix} s_{12}^2s_{13}^2 & \frac{1}{2}c_{12}s_{12}s_{13}^2 & 0 \\ \frac{1}{2}c_{12}s_{12}s_{13}^2 & 0 & 0 \\ 0 & 0 & -s_{12}^2s_{13}^2 \end{pmatrix}. \quad (3.8)$$

Due the different dependence of expansion parameters, one have terms like s_{13}^3 , $s_{13}r_\Delta$ and other have $s_{13}^2r_\Delta$. These Hamiltonians did not have any NSI.

Henceforth, our choice of the hierarchy can summarize as

1. the diagonal NSI elements, $\tilde{\epsilon}_{\alpha\alpha}$, are chosen to be included in the non-perturbated Hamiltonian;
2. the complex off-diagonal NSI parameters are to be considered sub-leading and sub-sub-leading;
 - the NSI coupling $\tilde{\epsilon}_{e\tau} \sim \sqrt{\kappa}$ is chosen to be included in first order of perturbed Hamiltonian;
 - the off-diagonal couplings $\tilde{\epsilon}_{e\mu} \sim \tilde{\epsilon}_{\mu\tau} \sim \kappa$, are chosen to be included in the high order in the perturbed Hamiltonian,

The full Hamiltonian \tilde{H} is given by

$$\tilde{H} = \tilde{H}^{(0)} + \tilde{H}^{(a)} + \tilde{H}^{(b)} + \tilde{H}^{(c)} + \tilde{H}^{(d)}, \quad (3.9)$$

The neutrino time-evolution Hamiltonian, \tilde{H} , as given in Eqs. (3.8-3.9), can now be evolved in time using the perturbation theory described in Appendix B. The desired probabilities can be written as

$$P(\nu_\alpha \rightarrow \nu_\beta) \equiv |S_{\beta\alpha}|^2, \quad (3.10)$$

where the S matrix is the neutrino evolution matrix given explicitly from Eq. (B.10).

When we do this computation, we get an infinite series for the probability. We are going to use *our choice of NSI hierarchies* to organize this series. The diagonal NSI elements are included in the non-perturbated Hamiltonian. Examples where you can this expression with diagonal NSI elements it are in Refs. [74–77]. As said before, the leading expansion parameter is (s_{13} and $\tilde{\epsilon}_{e\tau}$), and the next-leading parameters are r_Δ , $\tilde{\epsilon}_{e\mu}$ and $\tilde{\epsilon}_{\mu\tau}$. The first non-zero term that appear for $P(\nu_\mu \rightarrow \nu_e)$ probability is in first order of expansion (there is no zero-order contribution) depends on s_{13}^2 in the standard neutrino oscillation scenario, that came from the s_{13} dependence in the $\tilde{H}^{(a)}$. An explicit form for the muon neutrino to electron neutrino probability for the first order of expansion it given in the standard scenario in Ref. [30]. Physically speaking, this is related in the standard scenario with the *atmospheric oscillation* and the mixing angle θ_{13} relevant for long-baseline neutrino experiments. The dependence on r_Δ appear only at higher orders in the Hamiltonian $\tilde{H}^{(b)}$ that is connected with the so-called *solar oscillation* with the mixing angle θ_{12} , and which is subdominant for distances until 7000 km. This hierarchy used to have in the perturbative analytical solutions for the standard oscillation scenario. Now coming back to NSI, when we introduce the $\tilde{\epsilon}_{e\tau}$ parameter in $\tilde{H}^{(a)}$, this assumption means that $\tilde{\epsilon}_{e\tau}$ and the mixing parameter s_{13} will have the contribution for the same perturbation order. In other words, we will keep everywhere terms proportional to s_{13} and $\tilde{\epsilon}_{e\tau}$. Then, for the first order of perturbation theory, we expect to have terms like $|\tilde{\epsilon}_{e\tau}|^2$ and interference terms like $\tilde{\epsilon}_{e\tau} \times s_{13}$. The explicit expression for the the muon neutrino to electron neutrino probability

is given in [74–86]. For the other NSI parameters, our choice to have had them in $\tilde{H}^{(b)}$ it implies that we only appear in the second order in perturbation theory. For $\tilde{\epsilon}_{e\mu}$ the probability is listed in Refs. [74–86]. Finally, for $\tilde{\epsilon}_{\mu\tau}$ a form for this probability it appears in Ref. [30, 79].

In resume, to perform the perturbation theory, we notice that from the best fit values of mixing angle θ_{13} and the ratios of squared mass differences, we have an hierarchy between s_{13} and r_Δ , such that we can define the parameter κ as:

$$\sin^2 \theta_{13} \approx r_\Delta \approx 0.03 \rightarrow \kappa = 0.03. \quad (3.11)$$

Another point is what we call small or more significant for a NSI parameter. We will call the NSI parameters small when they are expected to be numerically (much) smaller than the unity. From the current bounds given in Eq. (1.12), we can see that this is the case for the parameters $\epsilon_{e\mu} \ll 1$, and $\epsilon_{\mu\tau} \ll 1$. However, the constrains over $\epsilon_{e\tau}$ are relatively weaker than the bounds over the other two non-diagonal NSI parameters. In fact, in this case we assume $\epsilon_{e\tau}^2 \ll 1$. The hierarchy of NSI parameters with respect to the parameter κ is then

$$\kappa \approx \epsilon_{\mu\tau}^{\text{small}} \approx \epsilon_{e\mu}^{\text{small}} \approx (\epsilon_{e\tau}^2)^{\text{small}}. \quad (3.12)$$

The explicit transformation of the NSI parameters from one basis to the other is given in Eq. (A.1). Furthermore, it is possible to see from Table 1 that Eq. (A.1) does not alter the hierarchy between the limits on the NSI parameters when we change from a basis to the other. In the same table we also include our assumption for the NSI hierarchy (also in the rotated basis $\tilde{\epsilon}_{\alpha\beta}$) given in the Eqs. (3.4 - 3.8). From a direct inspection, the last two columns of Table 1 it is possible to conclude that:

- For the parameters $\tilde{\epsilon}_{ee}$ and $\tilde{\epsilon}_{\tau\tau}$, our assumption covers all the allowed domain.
- Our premise for the hierarchy of the parameter $\tilde{\epsilon}_{e\tau}$ is that it is in the same order of magnitude than the current experimental bound at 3σ .
- For the parameters $\tilde{\epsilon}_{e\mu}$ and $\tilde{\epsilon}_{\mu\tau}$ our assumption on the NSI hierarchy is only one order of magnitude below the current limit at 3σ .

As already commented, the bounds from the literature assume that all NSI parameters, ϵ , are real. We can translate to ϵ' notation as defined in Eq. (1.5) and translated our bounds to $\epsilon'_{\alpha\beta}$, if we assume that there is no NSI with electrons: $\epsilon_{\alpha\beta}^{eV} = 0$.

Henceforth, from the above discussed in Table 1 and the associated text, we can expect that our resulting oscillation formulas are applicable in a full region of the current NSI allowed parameter space.

Moreover, we can characterize the different assumptions about NSI in two large categories:

1. include linear dependence of NSI off-diagonal elements [65, 79–86],
2. include NSI off-diagonal elements until second order, this work and Refs. [30, 73–77].

Parameter	3σ limit on $\epsilon_{\alpha\beta} \leq (\text{min:max})$	3σ limit translated to $\tilde{\epsilon}_{\alpha\beta}$	Our typical $\tilde{\epsilon}_{\alpha\beta}$
ϵ_{ee}	-0.65 : 1.40	-0.65 : 1.40	1.0
$\epsilon_{\tau\tau}$	-0.02 : 0.50	-0.06 : 0.29	0.5
$\epsilon_{e\tau}$	-1.10 : 0.43	-0.64 : 0.29	0.17
$\epsilon_{e\mu}$	-0.19 : 0.16	-0.14 : 0.46	0.03
$\epsilon_{\mu\tau}$	-0.05 : 0.04	-0.25 : 0.01	0.03

Table 1. Comparison between the limits on the NSI parameters, $|\epsilon_{\alpha\beta}| \leq (\text{min:max})$ given in Eq. (1.12), the same limits translated to the basis $\tilde{\epsilon}_{\alpha\beta}$ through Eq. (A.1) assuming $\theta_{23} = 45^\circ$, and the typical NSI values assumed in this work (also in the rotated basis $\tilde{\epsilon}_{\alpha\beta}$) given in Eqs. (3.4 - 3.8). Here we use all NSI parameters are real.

Parameter	This Work	[30]	[73]	[74–77]	[79]	[80–83]	[84–86]
s_{13}	4	4	2	2	2	2	2
r_Δ	2	2	2	2	2	2	2
ϵ_{ee}	all orders	1	–	all orders	1	–	–
$\epsilon_{\tau\tau}$	all orders	1	–	–	1	–	–
$\epsilon_{e\tau}$	4	2	2	1	1	1	1
$\epsilon_{e\mu}$	4	2	2	1	1	1	1
$\epsilon_{\mu\tau}$	1	1	–	–	1	–	–

Table 2. Comparison between the maximum order of the SO and NSI parameters that appears in our oscillation formulas, as it are given in Eqs. (4.2) and (4.5), and in the previous literature. The ” – ” notation means that the parameter is not present in the given formula.

Within these groups, we can have different assumption for the *diagonal NSI elements*, as follows: (i) we can have non-perturbative diagonal NSI as this work and Ref. [65, 79, 80], (ii) to have diagonal NSI parameters in first-order [30, 65, 73, 79, 80], and (iii) did not include diagonal NSI effect [81–86]. A disclaimer is that these different assumptions are justified in the respective works and inside their context all expansions are correct. What we want to point is that, given the present knowledge of upper bounds on the NSI elements, our assumptions are: to include the real NSI diagonal elements as non-perturbative and include a hierarchy of NSI parameters allow us to cover a wider range of NSI parameters and faithfully reproduce the numerical results of neutrino evolution. Another point is due to our choice of NSI hierarchy, and we can *reproduce* all perturbative models of neutrino probability as case limits of our expression. For example, if we keep only the first order of diagonal NSI elements in our results, we can reproduce Ref. [30].

4 Results for perturbation theory until second order in expansion parameter, κ^2

At this point we present our results for the neutrino oscillation probabilities obtained from perturbation theory described in Section 3. Explicitly, for the muon to electron-neutrino

oscillation case, each order of the oscillation probability is given by:

$$P^{(0)}(\nu_\mu \rightarrow \nu_e) = 0, \quad (4.1)$$

and,

$$P^{(1)}(\nu_\mu \rightarrow \nu_e) = 4 \frac{|\Sigma|^2 s_{23}^2}{r_A^2 \eta^2} \sin^2 \left(\frac{\Delta_{31} x}{2} r_A \eta \right), \quad (4.2)$$

and,

$$P^{(3/2)}(\nu_\mu \rightarrow \nu_e) = \frac{8c_{23}s_{23}|\Sigma||\Omega| \sin \left(\frac{\Delta_{31} x}{2} r_A \Gamma \right) \sin \left(\frac{\Delta_{31} x}{2} r_A \eta \right) \cos \left(\frac{\Delta_{31} x}{2} r_A \Lambda - \phi_\Sigma + \phi_\Omega \right)}{r_A^2 \Gamma \eta}, \quad (4.3)$$

and,

$$\begin{aligned} P^{(2)}(\nu_\mu \rightarrow \nu_e) = & \frac{4c_{23}^2 |\Omega|^2 \sin^2 \left(\frac{\Delta_{31} x}{2} r_A \Gamma \right)}{(r_A \Gamma)^2} \\ & + 2 |\Sigma|^2 s_{23}^2 \left(\frac{2 |\Sigma|^2}{r_A^3 \eta^3} - \frac{r_\Delta s_{12}^2 + 2s_{13}^2}{r_A^2 \eta^2} \right) (\Delta_{31} x) \sin(r_A \eta \Delta_{31} x) \\ & - 4s_{23}^2 \left(\frac{4 |\Sigma|^4}{r_A^4 \eta^4} - \frac{2 |\Sigma|^2 (r_\Delta s_{12}^2 + 2s_{13}^2)}{r_A^3 \eta^3} + \frac{|\Sigma| s_{13} (2r_\Delta s_{12}^2 + s_{13}^2) \cos(\delta_{\text{CP}} + \phi_\Sigma)}{r_A^2 \eta^2} \right) \\ & \times \sin^2 \left(\frac{\Delta_{31} x r_A \eta}{2} \right) + 4c_{23} |\tilde{\epsilon}_{\mu\tau}| |\Sigma|^2 s_{23} \sin \left(\frac{\Delta_{31} x}{2} r_A \eta \right) \\ & \times \left(\frac{\sin \left(\tilde{\phi}_{\mu\tau} - \frac{\Delta_{31} x r_A (\Gamma + \Lambda)}{2} \right)}{r_A^2 \eta \Gamma \Lambda} - \frac{\sin \left(\tilde{\phi}_{\mu\tau} - \frac{\Delta_{31} x r_A \eta}{2} \right)}{r_A^2 \eta^2 \Gamma} + \frac{\sin \left(\tilde{\phi}_{\mu\tau} + \frac{\Delta_{31} x r_A \eta}{2} \right)}{r_A^2 \eta^2 \Lambda} \right), \end{aligned} \quad (4.4)$$

where we have defined

$$\begin{aligned} \Sigma &= |\Sigma| e^{i\phi_\Sigma} \equiv s_{13} e^{-i\delta_{\text{CP}}} + r_A \tilde{\epsilon}_{e\tau}, \\ \Omega &= |\Omega| e^{i\phi_\Omega} \equiv r_\Delta c_{12} s_{12} + r_A \tilde{\epsilon}_{e\mu}, \\ \Lambda &\equiv \frac{1}{r_A} + \tilde{\epsilon}_{\tau\tau}, \\ \Gamma &\equiv (1 + \tilde{\epsilon}_{ee}), \\ \eta &\equiv \Lambda - \Gamma. \end{aligned} \quad (4.5)$$

Our *perturbative* probability it will be the sum of Eqs. (4.1-4.5), where Eq. (4.5) is implicitly assumed, which results in:

$$\begin{aligned} P^{\text{perturbative}}(\nu_\mu \rightarrow \nu_e) \equiv & P^{(0)}(\nu_\mu \rightarrow \nu_e) + P^{(1)}(\nu_\mu \rightarrow \nu_e) \\ & + P^{(3/2)}(\nu_\mu \rightarrow \nu_e) + P^{(2)}(\nu_\mu \rightarrow \nu_e). \end{aligned} \quad (4.6)$$

Our final result, Eq. (4.6), it is the perturbative solution for the full neutrino evolution equation and it is a power-law series of our expansion parameters, $(s_{13}, r_\Delta, \tilde{\epsilon}_{e\mu}, \tilde{\epsilon}_{e\tau}, \tilde{\epsilon}_{\mu\tau})$. Due to our choice of NSI hierarchy, we can rewrite as the combination $(\Sigma, \Omega, r_\Delta, \tilde{\epsilon}_{\mu\tau})$. We can related Σ and Ω with entries of perturbed Hamiltonian, $\tilde{H}^{(a)}$ and $\tilde{H}^{(b)}$. To obtain

the anti-neutrino oscillation probabilities, in Eq. (1.1) we change $U \rightarrow U^*$, $r_A \rightarrow -r_A$ and $\epsilon \rightarrow \epsilon^*$, whose implies in the modifications in the effective parameters given as

$$\begin{aligned}\Gamma &\rightarrow \Gamma, \\ \Sigma &\rightarrow \bar{\Sigma} = s_{13}e^{i\delta_{\text{CP}}} - r_A(\tilde{\epsilon}_{e\tau})^*, \\ \Omega &\rightarrow \bar{\Omega} = r_\Delta c_{12}s_{12} - r_A(\tilde{\epsilon}_{e\mu})^*.\end{aligned}\tag{4.7}$$

The formulas given by Eqs. (4.2-4.5) can be directly applied to any long-baseline experiment.

In Figure 1 we made the comparison of $P(\nu_\mu \rightarrow \nu_e)$ muon neutrino to electron neutrino for our results, shown in black line, given by Eq. (4.6) and compare with the results of other perturbative solutions present in the literature [30, 65, 73–77, 79–86]. We also compare it with the full numerical solution of neutrino evolution, shown in big dotted black curve, given in Eq. (1.3). For this figure we assume $L = 1300$ km and the matter density is assumed to be $\rho = 2.8$ g/cm³. We show in panel (a1), (c1), (e1) and (g1) the class of models of Ref. [30, 73] and in the panels (b1), (d1), (f1) and (h1) the class of models [65, 74–77, 79–86] with different color lines as shown in Figure 1.

The relative difference between the full numerical solution and the different analytical models are defined by

$$R = \frac{P^{\text{model}} - P^{\text{numerical}}}{\bar{P}^{\text{numerical}}},\tag{4.8}$$

where P^{model} is the oscillation probability for different perturbation theory scenarios presented in Table 2, $P^{\text{numerical}}$ is the full numerical computation and \bar{P} represents the mean probability in nearest neutrino bin energies³. We showed in Figure 1, the ratio R in the panel (a2) that correspond to the models shown in the panel (a1). The same applies for the other panels (b2), (c2), (d2), (e2), (f2), (g2), and (h2). Let us first comment on panel (a2). All curves agree with the numerical computation for energies above 1 GeV. The region below 1 GeV is where it happens the stronger effects of the *solar scale* for long-baseline experiments, and this disagreement is known already. Nowadays, we know that this is related to the standard oscillation scenario, and here we will refer only to the results for energies above 1 GeV. For the other panels, we choose values of NSI parameters that can exemplify better the range of applicability of different perturbative solutions of the neutrino probability. If we follow our results, shown by the black curve in all panels showing the ratio R , we can notice it have the better agreement with respect with all other curves for any of the set of the NSI parameters chosen. In the intermediate panels (a2) and (b2), the ratio R corresponds to what we define as *small* NSI parameters; our results are equal or better than the other perturbative series. When we increase the diagonal NSI element, which differentiates the models as well in the Table 2, the panel (c2) and (d2) show that our results still can reproduce the numerical results, smaller R , and the others begin to deviate more badly from the numerical solution reaching a $R \sim 20\%$. For the panels (e2) and (f2), we have shown the results for larger values of non-diagonal NSI parameters,

³Strictly speaking, we applied the median filter from Python [121]. The averaging procedure is used to avoid divergences in the ratio of R when the numerical probability has a local minimum.

where we assume to be real, $\epsilon_{e\mu} = 0.1$ and $\epsilon_{e\tau} = 0.2$, but still, our computation have a much better agreement. For even larger values of, where we assume to be real, $\epsilon_{e\mu} = 0.1$ and $\epsilon_{e\tau} = 0.5$, shown in the panels (g2) and (h2) we can begin to notice in there are models with $R \sim 30\%$. The summary is that for any of these choices of NSI parameters, we can have a better agreement than any other model with the numerical results of the neutrino probability.

The same approach within perturbation theory can be applied to calculate muon neutrino survival probability. In Appendix C we show our results for muon neutrino probability $P^{\text{perturbative}}(\nu_\mu \rightarrow \nu_\mu)$ in the perturbative approach.

5 Study of degeneracies in the neutrino probability

As mentioned in Section 2, it was found that in both standard scenarios as well as in the NSI scenario that we can have multiple solutions of the parameters that led to the same the neutrino oscillation probability. Examples of this are in Ref. [44], where the neutrino oscillation probability calculated numerically and that it will be relevant later. Another example is when in Ref. [73], it was analyzed the conditions for *matter hesitation* when the NSI neutrino probability has the same value as the vacuum standard oscillation probability.

Here, we choose to use the advantage of having an analytical expression for neutrino probability and use this to understand the root of the neutrino probability degeneracy. The degeneracy studied in the literature can be classified in the three categories:

1. when it involve only standard oscillation parameters,

$$[P(\nu_\alpha \rightarrow \nu_\beta)(\Delta m_{ij}^2, \theta_{ij})]^{(\text{SO})} = [P(\nu_\alpha \rightarrow \nu_\beta)(\Delta m_{ij}^2, \theta_{ij})]^{(\text{SO})}, \quad (5.1)$$

where $[P(\nu_\alpha \rightarrow \nu_\beta)(\Delta m_{ij}^2, \theta_{ij})]^{(\text{SO})}$ is the three-neutrino standard neutrino probability for a given set of mixing angle parameters $(\Delta m_{ij}^2, \theta_{ij})$ and $(\Delta m_{ij}^2, \theta_{ij})$ are different set of parameters. One example where this equation it is fulfilled is a special case of the generalized mass ordering degeneracy for null NSI parameters [44], as mentioned in Section 1. It is the so called matter hesitation phenomena, where the neutrino probability in matter have the same dependence with energy as it was in vacuum. It is an example of this equality expressed in Eq. (5.1) and it was first discussed in Ref. [73]. We will not consider the degenerescence type I, as they have been discussed elsewhere.

2. a second case it is when it involves only NSI parameters,

$$[P(\nu_\alpha \rightarrow \nu_\beta)(\tilde{\epsilon}_{\alpha\beta}, \Delta m_{ij}^2, \theta_{ij})]^{(\text{NSI})} = [P(\nu_\alpha \rightarrow \nu_\beta)(\tilde{\epsilon}_{\alpha\beta}, \Delta m_{ij}^2, \theta_{ij})]^{(\text{NSI})}, \quad (5.2)$$

where $[P(\nu_\alpha \rightarrow \nu_\beta)(\tilde{\epsilon}_{\alpha\beta}, \Delta m_{ij}^2, \theta_{ij})]^{(\text{NSI})}$ is the neutrino probability in the NSI scenario, $\tilde{\epsilon}_{\alpha\beta}$ and $\tilde{\epsilon}_{\alpha\beta}$ are two different set of NSI parameters. One example of this behaviour was shown in Ref. [90]. This is the more oversight case in the literature

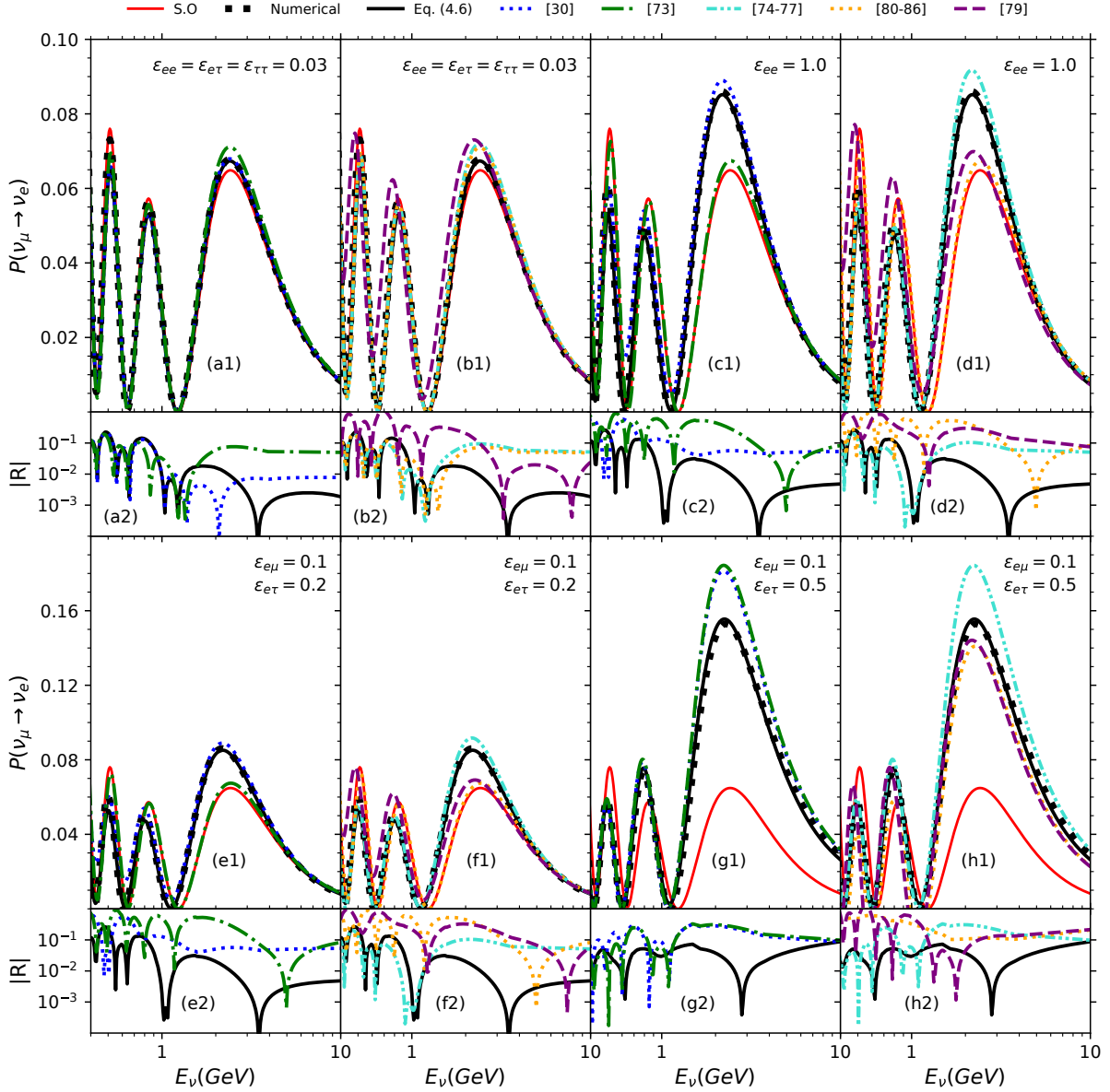


Figure 1. Panels (a1), (b1), (c1), (d1), (e1), (f1), (g1), (h1): Comparison between the numerical solution and the results from perturbation theory for neutrino oscillation probability. Our perturbative solution (solid black curve) is obtained using Eq. (4.6) and our numerical results are represented by the big dotted black curve. Also, the standard oscillation solution is shown by the solid cyan curve. Other colored dashed lines refers to the predictions from the Refs. quoted in Table (2). **Panels (a2), (b2), (c2), (d2), (e2), (f2), (g2), (h2):** The ratio of probabilities as it is given in Eq. (4.8) for the respective NSI values assumed in the panels (a1), (b1), (c1) and (d1). Notice the change in the scale of the plots in the upper/lower panel. We assume the values of mixing angles given in the text and $L=1300\text{km}$. All NSI parameters are assumed to be real.

and it can have impact on the understand of the future results of neutrino oscillations. We will discuss later in detail in Section 5.1 and in the respective Figures 2,

3, and 4, the source of this behaviour using our perturbative formulas.

3. when is due to the standard oscillation parameters and NSI parameters. Respectively

$$[P(\nu_\alpha \rightarrow \nu_\beta)(\tilde{\epsilon}_{\alpha\beta}, \Delta m_{ij}^2, \theta_{21}, \theta_{13}, \boldsymbol{\theta}_{23})]^{(\text{NSI})} = [P(\nu_\alpha \rightarrow \nu_\beta)(\tilde{\epsilon}_{\alpha\beta} = 0, \Delta m_{ij}^2, \theta_{21}, \theta_{13}, \theta_{23})]^{(\text{SO})}, \quad (5.3)$$

where $[P(\nu_\alpha \rightarrow \nu_\beta)(\tilde{\epsilon}_{\alpha\beta}, \Delta m_{ij}^2, \theta_{21}, \theta_{13}, \boldsymbol{\theta}_{23})]^{(\text{NSI})}$ is the neutrino oscillation probability in the NSI scenario, $[P(\nu_\alpha \rightarrow \nu_\beta)(\tilde{\epsilon}_{\alpha\beta} = 0, \Delta m_{ij}^2, \theta_{21}, \theta_{13}, \theta_{23})]^{(\text{SO})}$ is the neutrino oscillation probability in the standard scenario. Here $\boldsymbol{\theta}_{ij}$ and θ_{ij} are two different values for each mixing angle $i, j=1, 2, 3$. This example of degenerescence was discussed in many situations, one was the so called *dark solution for the solar neutrino problem* [89]. It was generalized for any oscillation scenario in Ref. [44]. We will discuss it in Section 5.2 and Figure 5.

Furthermore, in the NSI scenario, the parameters which describe the neutrino oscillation are:

1. Standard Oscillation parameters: six SO parameters (the three mixing angles θ_{12} , θ_{13} , θ_{23} , the two squared mass differences, Δm_{21}^2 and Δm_{31}^2 , and the CP phase, δ_{CP}),
2. Non-Standard Oscillation parameters: two real parameters, ϵ_{ee} , and $\epsilon_{\tau\tau}$ and three complex parameters $\epsilon_{e\mu}$, $\epsilon_{e\tau}$, and $\epsilon_{\mu\tau}$,

and then we have in total fourteen parameters. When perturbation theory is applied to solve Eq. (1.1), we can describe the neutrino oscillation probability as function of

1. the parameters, $(\Lambda, \Gamma, \Sigma, \Omega)$ given in Eq. (4.5),
2. the parameter $\epsilon_{\mu\tau} = |\epsilon_{\mu\tau}|e^{i\phi_{\mu\tau}}$,
3. the parameters s_{13} , s_{12} , s_{23} and, Δ_{31} and, r_Δ ,

and then we have eleven free parameters in this framework.

There are in the literature distinct theoretical works where the degeneracy problem was studied. Noticeable examples are in Refs. [65, 74, 78, 84, 85], where the degeneracy between NSI parameters and different mixing parameters are studied. Indeed, in Ref. [74] it is assumed the real parameter $\epsilon_{ee} \in H^{(0)}$ and the interplay between δ_{CP} and $\epsilon_{e\mu}$ and the magnitude of complex parameter $|\epsilon_{e\tau}|$ is considered in the calculation of DUNE sensitivities. Our Eqs. (5.14, 5.15, 5.17) present a similar relation between the above mentioned NSI parameters and the standard oscillation parameters, as it can be verified in the Eqs. (C1, C2) of [78] and the associated text. In Ref. [84], the resulting oscillation formula presented in their Eq. (12) depends on explicitly combinations of δ_{CP} and the phases associated with the parameters that are considered with order of the magnitude of NSI parameters $|\epsilon_{e\mu}|, |\epsilon_{e\tau}| \leq 0.1 \approx \sqrt{\kappa}$. All the other NSI parameters are assumed to the order κ and the impact on the DUNE sensitivities to the δ_{CP} is calculated. In Ref. [85] the authors assume the neutrino oscillation probabilities given in Refs. [63, 111, 122] and calculate the DUNE

sensitivities in terms that are odd and even terms with respect to δ_{CP} . In Ref. [86] a similar procedure is used to determine DUNE sensitivities to the neutrino mass hierarchy. Additionally, combinations of $\delta_{\text{CP}} + \text{NSI}$ phases also appear in the results in Ref. [65].

Moreover, in the sensitivity studies in the plane of the NSI parameters; it appears as multiple solutions in numerical computations. One example, in Ref. [68], in the plane $|\epsilon_{e\tau}| \times \epsilon_{ee}$ there are two branches of solutions, *butterfly* like and also $\epsilon_{\tau\tau} \times \epsilon_{\mu\tau}$ plane. Similarly, multiple solutions found in Ref. [44]. One set of solutions is compatible with *small* NSI parameters, but also it has a puzzling behavior *large* NSI parameters that also are compatible. In these sensitivity studies, they compute the rate of events in the case of standard oscillation probability and compare with the NSI probability. Due to this, we were motivated to ask if the perturbation theory can explain (or at least mimic) the existence of these multiple solutions.

To answer such question, in what follows, we will use oscillation formulas within perturbation theory in two different ways:

- Perform a graphic comparison between perturbative solutions between different NSI assumptions,
- Find analytic expressions for the neutrino probability degenerescence from Eqs. (4.5-4.5).

5.1 Degenerescence type 2, only NSI parameters

As a matter of illustration of such degenerate behavior of neutrino time evolution Hamiltonian, in the panels of Figure 2 where we show the effect of the diagonal NSI ϵ_{ee} parameter and the non-diagonal NSI parameter, which we assume to be real for this figure, $\epsilon_{e\tau}$. In panels (a1), (b1) and (c1), we show the muon neutrino to electron neutrino conversion. In panels (a2), (b2) and (c2) we graph the quantity

$$Q = \frac{P^{\text{NSI}} - P^{\text{SO}}}{\bar{P}^{\text{SO}}}, \quad (5.4)$$

that was calculated in the same way as in Eq. (4.8). Nevertheless, now, we have P^{NSI} that refers to Eq. (4.6) including the respective non-standard interaction, and P^{SO} is the same equation in the standard oscillation scenario.

We noticed in the left (middle) panel of Figure 2 that due to, assumed real parameter, $\epsilon_{e\tau} > 0$ ($\epsilon_{ee} < 0$) has the effect to decrease (increase) of the oscillation amplitude. For this set of parameters, when the only non-zero parameters are, assumed here to be real, $\epsilon_{e\tau}$ and ϵ_{ee} , we have

$$\tilde{\epsilon}_{\mu\mu} = \tilde{\epsilon}_{\tau\tau} = \tilde{\epsilon}_{\mu\tau} = 0; \quad \tilde{\epsilon}_{e\mu}, \tilde{\epsilon}_{e\tau}, \tilde{\epsilon}_{ee} \neq 0. \quad (5.5)$$

From Eq. (4.5) and Eq. (5.5) implies that

$$\Omega \rightarrow \frac{1}{r_A}; \quad \Gamma \rightarrow 1 + \epsilon_{ee}; \quad \eta = \frac{1}{r_A} - (1 + \epsilon_{ee}); \quad \Sigma \sim r_A c_{23} \epsilon_{e\tau}; \quad \Omega \sim -r_A s_{23} \epsilon_{e\tau}.$$

Then if, assumed to be here a real parameter, $\epsilon_{e\tau} > 0$ ($\epsilon_{ee} < 0$) implies a larger $\Sigma(\eta)$. From the neutrino probability in the first order, Eq. (4.3), larger $\Sigma(\eta)$ implies in a smaller

(larger) amplitude of neutrino oscillation. For lower values of energy, the high orders of the perturbation theory are important and they depend also on Ω that have a different energy dependence from Σ . Then even one single NSI parameter can have opposite effects in the oscillation probability and can indicate that the combined effect of more than one NSI can cancel the NSI effect. To illustrate that, in the right panel of Figure 2 we show two cases where ϵ_{ee} and $\epsilon_{e\tau}$ are intentionally large and with opposite signs. In this situation for both non-zero, it happens that Σ and η decrease (increase) when $\epsilon_{e\tau}$ and ϵ_{ee} have opposite signs as you can see in Eq. (5.1), and for a particular choice we can have

$$|\Sigma| \sim |\eta|. \quad (5.6)$$

Also, small η values do not change the phase of neutrino oscillation (that translate into the condition $\epsilon_{ee} < 1$). As one can see, in this situation we have the canceling the NSI effects in Eq. (4.3). For lower energies, the contribution of high orders is more important and the effects of Ω are important and there is no canceling effects. In what follows, we apply

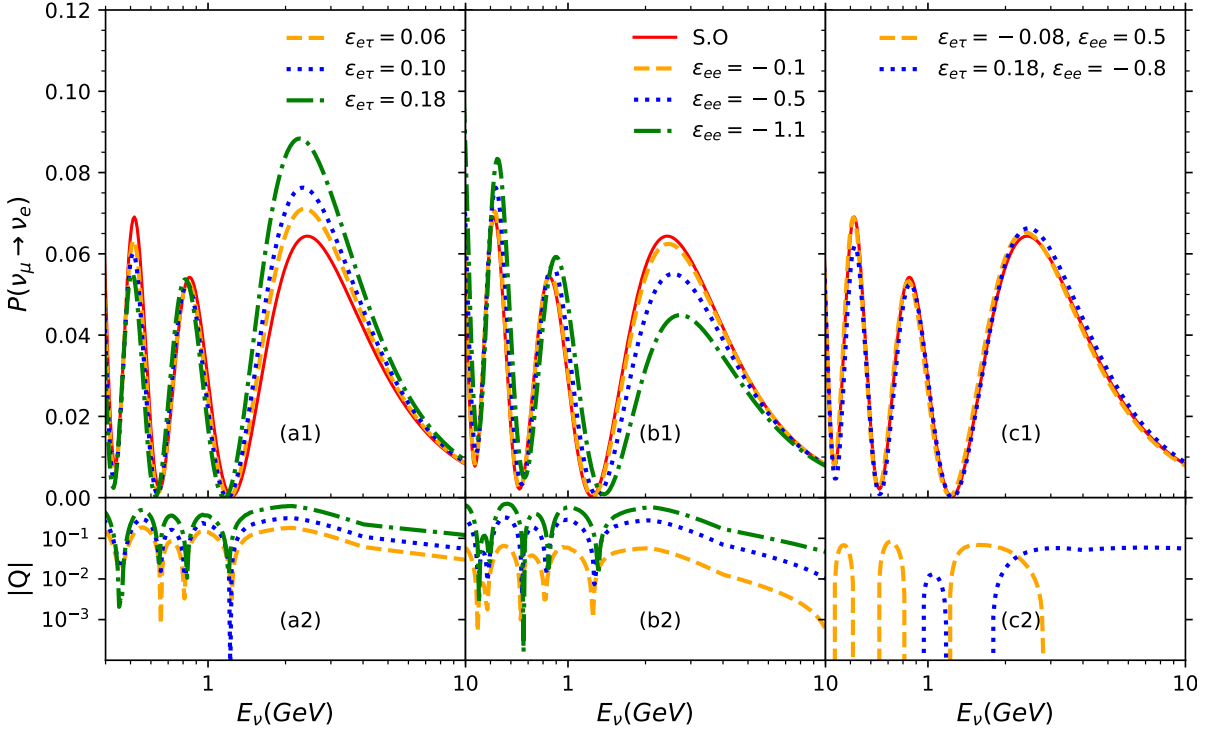


Figure 2. Panels (a1), (b1), (c1): Comparison between our analytical solution for the oscillation probabilities, $P(\nu_\mu \rightarrow \nu_e)$, for the SO (solid line) case and different sets of ϵ_{ee} and $\epsilon_{e\tau}$ NSI parameters (dotted and dotted-dashed lines). In panel (a1) we show the SO prediction and three NSI cases where only $\epsilon_{e\tau}$ is non-zero and assumes the values indicated in the plot. In panel (b1) we show SO prediction and three cases where only ϵ_{ee} is non-zero. In panel (c1) we show SO prediction and two cases where only ϵ_{ee} and $\epsilon_{e\tau}$ are non-zero and with opposite sign. **Panels (a2), (b2), (c2):** We shown the ratio Q as it is given in Eq. (5.4) for the correspondent curves quoted in panels (a1), (b1), (c1). We assume in this plot that all NSI parameters are real.

the perturbation theory to determine analytically the origin of the neutrino oscillation probabilities degenerescence.

5.2 Degenerescence type 3, standard oscillation mixing parameters and NSI parameters

Although it is relatively easy to obtain the numerical solutions of Eq. (1.1), it is not straightforward to establish a cause-effect relationship for the given NSI parameters and the resulting modifications in the behavior of the neutrino time evolution. Henceforth, our formalism within perturbation theory can be used to interpret the resulting neutrino oscillation probabilities. To get the information about the sources of the degenerate solutions for the neutrino probability we are going to use the fact that the two-neutrino flavor oscillation formula,

$$P_{\text{conversion}}^{2\nu} = \sin^2 2\theta \times \sin^2 \left(\frac{\Delta m^2 L}{4E_\nu} \right), \quad (5.7)$$

and the first order of the perturbative series $P^{(1)}(\nu_\mu \rightarrow \nu_e)$ can be cast into a similar format

$$P^{(1)}(\nu_\mu \rightarrow \nu_e) = A^{(1)}(\nu_\mu \rightarrow \nu_e) \times \sin^2(\Phi^{(1)}(\nu_\mu \rightarrow \nu_e)), \quad (5.8)$$

where $A^{(1)}(\nu_\mu \rightarrow \nu_e)$ is the oscillation amplitude and $\Phi^{(1)}(\nu_\mu \rightarrow \nu_e)$ is the phase.

First of all, let us assume that NSI parameters are zero, $\tilde{\epsilon}_{\alpha\beta} = 0$ in Eq. (4.2), then we have the standard oscillation formula in our approach,

$$\left[P^{(1)}(\nu_\mu \rightarrow \nu_e) \right]^{(\text{SO})} = \left[A^{(1)}(\nu_\mu \rightarrow \nu_e) \right]^{(\text{SO})} \sin^2 \left(\frac{\Delta_{31} x}{2} (1 - r_A) \right), \quad (5.9)$$

where

$$\left[A^{(1)}(\nu_\mu \rightarrow \nu_e) \right]^{(\text{SO})} = \frac{4s_{13}^2 s_{23}^2}{(1 - r_A)^2}, \quad (5.10)$$

that correspond to the first term of the expansion of the probability for the mixing parameter θ_{13} .

When we switched on the diagonal NSI parameters that enter in $\tilde{H}^{(0)}$, then Eq. (4.2) can be recast as

$$\begin{aligned} \left[P^{(1)}(\nu_\mu \rightarrow \nu_e) \right]^{(\text{diagonal NSI})} &= \left[A^{(1)}(\nu_\mu \rightarrow \nu_e) \right]^{(\text{diagonal NSI})} \\ &\times \sin^2 \left[\Phi^{(1)}(\nu_\mu \rightarrow \nu_e) \right]^{(\text{diagonal NSI})}, \end{aligned} \quad (5.11)$$

where

$$\begin{aligned} \left[A^{(1)}(\nu_\mu \rightarrow \nu_e) \right]^{(\text{diagonal NSI})} &= \frac{4s_{13}^2 s_{23}^2}{[1 - r_A + r_A(\tilde{\epsilon}_{\tau\tau} - \tilde{\epsilon}_{ee})]^2}, \\ \left[\Phi^{(1)}(\nu_\mu \rightarrow \nu_e) \right]^{(\text{diagonal NSI})} &= \frac{\Delta_{31} x}{2} [1 - r_A + r_A(\tilde{\epsilon}_{\tau\tau} - \tilde{\epsilon}_{ee})]. \end{aligned} \quad (5.12)$$

Comparing Eq. (5.10) and Eq. (5.12), we have

$$\begin{aligned}\frac{[A^{(1)}(\nu_\mu \rightarrow \nu_e)]^{(\text{SO})}}{[A^{(1)}(\nu_\mu \rightarrow \nu_e)]^{(\text{diagonal NSI})}} &= (1 + \gamma)^2, \\ \frac{[\Phi^{(1)}(\nu_\mu \rightarrow \nu_e)]^{(\text{SO})}}{[\Phi^{(1)}(\nu_\mu \rightarrow \nu_e)]^{(\text{diagonal NSI})}} &= \frac{1}{(1 + \gamma)},\end{aligned}\tag{5.13}$$

where we define real parameter γ

$$\gamma \equiv \frac{r_A (\tilde{\epsilon}_{\tau\tau} - \tilde{\epsilon}_{ee})}{1 - r_A}.$$

Now, we are switched on all NSI parameters, and we arrive to

$$\begin{aligned}\frac{[A^{(1)}(\nu_\mu \rightarrow \nu_e)]^{(\text{diagonal NSI})}}{[A^{(1)}(\nu_\mu \rightarrow \nu_e)]^{(\text{NSI})}} &= \frac{1}{1 + a(a + 2 \cos(\zeta))}, \\ \frac{[\Phi^{(1)}(\nu_\mu \rightarrow \nu_e)]^{(\text{diagonal NSI})}}{[\Phi^{(1)}(\nu_\mu \rightarrow \nu_e)]^{(\text{NSI})}} &= 1,\end{aligned}\tag{5.14}$$

where the parameter a is defined as,

$$a \equiv \frac{r_A}{s_{13}} |\tilde{\epsilon}_{e\tau}|,\tag{5.15}$$

and we define ζ ,

$$\zeta \equiv \delta_{\text{CP}} + \tilde{\phi}_{e\tau} = \phi_\Sigma,\tag{5.16}$$

where the angle ζ , it is a combination of the CP phase, δ_{CP} , and the NSI phase from $\tilde{\epsilon}_{e\tau}$. It is equal to the phase of Σ parameter defined in Eq. (4.5), $\Sigma = |\Sigma|e^{i\phi_\Sigma}$. Notice that in Eq. (5.14) the modification in the oscillation amplitude due to the inclusion of NSI depends only the net phase ζ , and does not depend on each phase individually. Indeed, also the oscillation probabilities given by Eqs. (4.2 and 4.3) depend only the phase ζ . Similar dependence on the sum of δ_{CP} and NSI phases was found in the Ref. [65]. Furthermore, from Eqs. (5.13-5.14) one can determine the impact of NSI until first order in perturbation theory simply as

$$[A^{(1)}(\nu_\mu \rightarrow \nu_e)]^{(\text{NSI})} = \frac{1 + a(a + 2 \cos(\zeta))}{(1 + \gamma)^2} [A^{(1)}(\nu_\mu \rightarrow \nu_e)]^{(\text{SO})},\tag{5.17}$$

and

$$[\Phi^{(1)}(\nu_\mu \rightarrow \nu_e)]^{(\text{NSI})} = (1 + \gamma) [\Phi^{(1)}(\nu_\mu \rightarrow \nu_e)]^{(\text{SO})}.\tag{5.18}$$

The Eqs. (5.17) and (5.18) summarizes the modifications respectively in the terms of the amplitude $[A^{(1)}(\nu_\mu \rightarrow \nu_e)]$ and the phase $[\Phi^{(1)}(\nu_\mu \rightarrow \nu_e)]$ due to the inclusion of the NSI parameters that are present in Eq. (4.2). In what follow we investigate how our formalism within perturbation theory can be used to determine the origin of the degenerate behavior of neutrino time-evolution.

The respective constraints over the standard oscillation and NSI parameters can be obtained from the Eq. (5.17) and Eq. (5.18). The conditions for both oscillation amplitude and phase to be degenerated implies in:

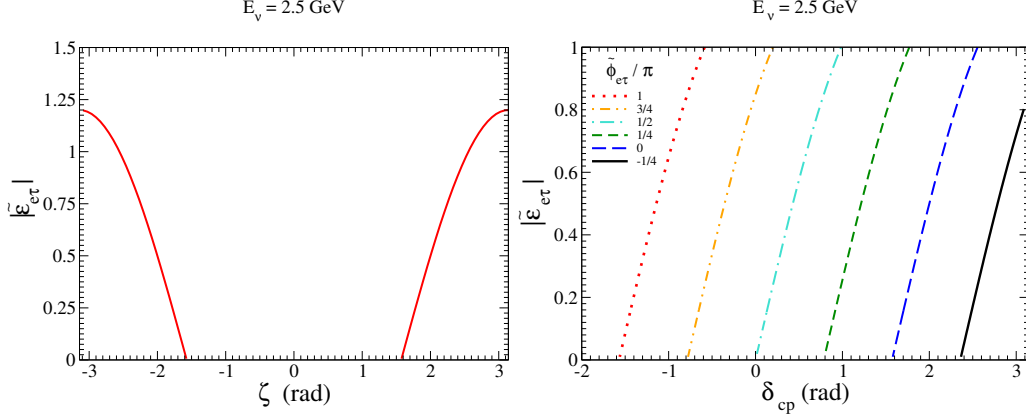


Figure 3. Left (right) panel:, possible combinations of ζ and $|\tilde{\epsilon}_{e\tau}|$ (δ_{CP} and the amplitude of the NSI parameter $|\tilde{\epsilon}_{e\tau}|$) that lead to $[P^{(1)}(\nu_\mu \rightarrow \nu_e)]^{(\text{SO})} = [P^{(1)}(\nu_\mu \rightarrow \nu_e)]^{(\text{NSI})}$. We assume all NSI parameters to be real. From the left-to-right we have decreasing values of phase $\tilde{\phi}_{e\tau}$ of the NSI element $\tilde{\epsilon}_{e\tau}$.

1. equal oscillation amplitude: from Eq. (5.17), $\gamma \rightarrow 0$
2. equal oscillation phase: from Eq. (5.18), $a + 2\cos(\zeta) \rightarrow 0$,

where the first and second condition implies that the following condition on the real diagonal NSI parameters (i)

$$\tilde{\epsilon}_{\tau\tau} = \tilde{\epsilon}_{ee}, \quad (5.19)$$

and (ii)

$$|\tilde{\epsilon}_{e\tau}| = -2 \frac{s_{13}}{r_A} \cos \zeta. \quad (5.20)$$

Both conditions warrant that the phase and the amplitude are equal for the SO oscillation and the SO \otimes NSI cases, for a given energy and when the first term of perturbative expansion is dominant. In the left (right) panel of Figure 3 we present the values in the plane $\tilde{\epsilon}_{e\tau} \times \zeta$ ($\tilde{\epsilon}_{e\tau} \times \delta_{\text{CP}}$). We use Eqs. (5.17, 5.18), where the conditions given in Eqs. (5.19, 5.20) are obeyed, in such way that always we can find a solution for any $\tilde{\epsilon}_{e\tau}$. Notice that in the standard neutrino oscillation perturbation expansion, the first term of the expansion is independent of the CP violation, δ_{CP} , and here due to the NSI interference we are not sensitive to CP violation even at leading order.

Even more, from our results given in Figures 1 and 2, we can see that, for the DUNE case, the amplitude of neutrino oscillation tends to be more sensitive to the NSI than the oscillation phase. If we impose the condition

$$\left[A^{(1)}(\nu_\mu \rightarrow \nu_e) \right]^{(\text{NSI})} = \left[A^{(1)}(\nu_\mu \rightarrow \nu_e) \right]^{(\text{SO})}, \quad (5.21)$$

then this implies that from Eq. (5.17) we define an effective phase ζ' as

$$\cos \zeta' = \frac{(1 + \gamma)^2 - 1 - a^2}{2a}, \quad (5.22)$$

that it is written as function of γ from from Eq. (5.14) and a from Eq.(5.15). The Eq. (5.22)

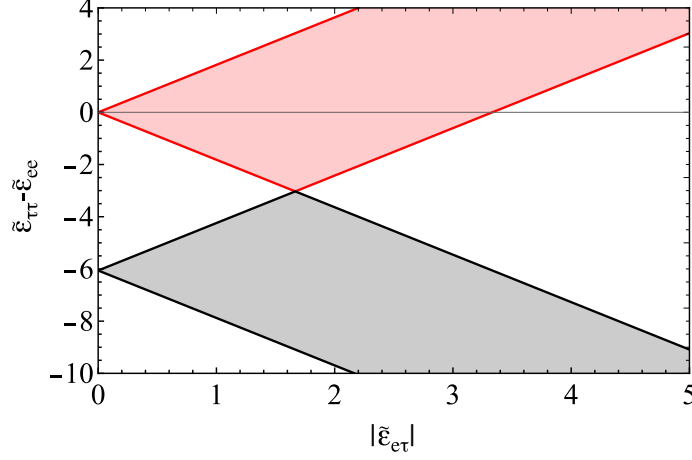


Figure 4. Region in the phase-space of the magnitude of $|\tilde{\epsilon}_{e\tau}|$, $\tilde{\epsilon}_{ee}$ and $\tilde{\epsilon}_{\tau\tau}$ that lead to have the same amplitudes $[A^{(1)}(\nu_\mu \rightarrow \nu_e)]^{(\text{NSI})} = [A^{(1)}(\nu_\mu \rightarrow \nu_e)]^{(\text{SO})}$. The non-diagonal NSI element, $\tilde{\epsilon}_{e\tau}$ can be complex.

relate the variables, $\tilde{\epsilon}_{e\tau}, \tilde{\epsilon}_{ee}, \tilde{\epsilon}_{\tau\tau}$ and ζ . By requiring that $-1 \leq \cos(\zeta) \leq +1$ we found the conditions for the degeneracy in the amplitude happens if,

$$\begin{aligned} |1 - a| - 1 &\leq \gamma' \leq a, \\ -(1 + a) - 1 &\leq \gamma' \leq -|1 - a| - 1. \end{aligned} \quad (5.23)$$

The four conditions, due to the possibility to have $a > 1$ or $a < 1$, presented in Eq. (5.23), define a region of the phase-space where the amplitude of standard oscillation is degenerated with NSI in the plane of $\tilde{\epsilon}_{e\tau}, \tilde{\epsilon}_{ee}, \tilde{\epsilon}_{\tau\tau}$. Then *we have found conditions to have the neutrino probability degeneracy between the standard neutrino scenario and the NSI scenario*. The results are presented in Figure 4, where we can conclude that depending on the relative signal of $\tilde{\epsilon}_{\tau\tau} - \tilde{\epsilon}_{ee}$ and the values of $\tilde{\epsilon}_{e\tau}$ we can have a complete canceling of the NSI effect. Then we have shown that we can have the cancellation of the NSI effect as exact for the first order of the perturbation theory. Higher-order effects of the perturbation theory can spoil the neutrino probability degenerescence.

5.2.1 Degenerescence type 3, assuming different mixing angles

Until now, we have assumed that the equality of probabilities for the same values of the mixing angles. For example, Eqs. (5.17), (5.18), and (5.21), and Figure 2. Nevertheless, in the phenomenological analysis of the constraints on NSI parameters, we marginalized over the mixing parameters to show the constraints in the plane of NSI variables and then the degeneracy came from not from equality of probabilities in standard neutrino case and with NSI with *the same* mixing angles. One example of an analysis of the sensitivity of DUNE for NSI in the plane of $\epsilon_{e\tau} \times \epsilon_{ee}$ is Ref. [44]. In this work [44], it has marginalized overall mixing angles not shown in the plot. In this reference, one of the plots shown, reproduced

in Figure 5, shows the blue region, going from darker blue, intermediate blue and lighter blue we have respectively 1σ , 2σ and 3σ allowed regions.

We will try to understand this behaviour using our formalism of perturbation theory for NSI. We will assume that

$$[P(\nu_\alpha \rightarrow \nu_\beta)(\tilde{\epsilon}_{\alpha\beta}, \theta_{23})]^{(\text{NSI})} = [P(\nu_\alpha \rightarrow \nu_\beta)(\tilde{\epsilon}_{\alpha\beta} = 0, \theta_{23})]^{(\text{SO})}, \quad (5.24)$$

where for *right side of this equality* the standard oscillation case, we will fix the mixing angle θ_{23} at the best-fit point of Ref. [123], and for *the left side of this equality* we will assume a different angle θ_{23} . We will search for these solutions of this equality, assuming a fixed θ_{23} and changing θ_{23} inside the 3σ allowed region [123]. A non-zero NSI will change the neutrino probability and we will search if we can use a different value of mixing angle θ_{23} , such that the value of NSI probability became equal to standard neutrino oscillation probability.

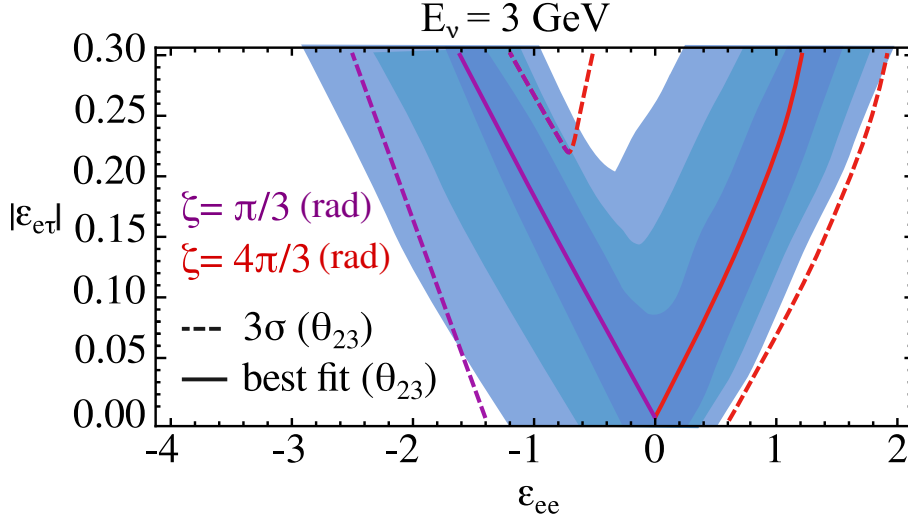


Figure 5. Superposition of our iso-probabilities (lines) from Eq. (5.25) with the allowed region in the plane ϵ_{ee} and the amplitude $|\epsilon_{e\tau}|$ (shaded region) reported in Ref. [44]. In this region, color darkness refers to the $(1\sigma, 2\sigma, 3\sigma)$ regions the authors found in their sensitivity study of the DUNE experiment. Solid (dashed) red curves are generated using the best-fit point for θ_{23} , $s_{23}^2 = 0.441$ and for combined phase $\zeta = 4\pi/3$ (rad) (the 3σ values $s_{23}^2 = 0.385 \rightarrow 0.635$). The solid (dashed) magenta curves have the same respective θ_{23} values but the phase ζ is equal to $\zeta = \pi/3$ (rad). Both values for θ_{23} are from Ref. [123].

We can rewrite the Eq. (5.24), using the explicit forms for the neutrino probability, as given in Eq. (4.2). After some algebra, discussed in detail in Appendix D we arrive to the expression

$$\frac{r_A^2}{s_{13}^2} |\tilde{\epsilon}_{e\tau}|^2 + 2 \frac{r_A}{s_{13}} |\tilde{\epsilon}_{e\tau}| \cos(\zeta) + 1 = \left(\frac{s_{23}}{s_{23}} \right)^2 \left(\frac{B_1}{B_1 + B_2 r_A (\tilde{\epsilon}_{\tau\tau} - \tilde{\epsilon}_{ee})} \right)^2, \quad (5.25)$$

where $s_{23} \equiv \sin(\theta_{23})$ is the value for θ_{23} for NSI neutrino probability in Eq. (5.24), θ_{23} used in the standard neutrino probability and B_1 and B_2 are defined in the Appendix D.

The Eq. (5.25) expresses the condition to have equality between the standard neutrino oscillation and the NSI probability given in Eq. (5.24) in terms of δ_{CP} , θ_{23} the complex parameter $|\tilde{\epsilon}_{e\tau}|$, $\tilde{\epsilon}_{ee}$, $\tilde{\epsilon}_{\tau\tau}$ and the phase $\zeta = \tilde{\theta}_{e\tau} + \delta_{\text{CP}}$. It also depends on the effective matter potential that neutrino crosses and the neutrino energy, which is contained in r_A parameter. Concerning an example DUNE distance of $L=1300$ km, in Figure 5, we show the iso-probability curves (solution of Eq. (5.25)) for the parameters ϵ_{ee} and $\epsilon_{e\tau}$, assuming all other NSI parameters to be zero. We plot

1. solving Eq. (5.25), assuming values for θ_{23} , s_{23} equal to best fit values. This implies that $s_{23} = s_{23}$. We assume that for combined phase $\zeta = 4\pi/3(\pi/3)(\text{rad})$ and we got the solid red (violet) curve respectively,
2. solving Eq. (5.25), assuming values s_{23} inside the 3σ allowed values of θ_{23} . Again the solid red (violet) curve respectively for combined phase $\zeta = 4\pi/3(\pi/3)(\text{rad})$.

The results of sensitivity for the NSI calculation for the DUNE experiment [44], are shown in Figure 5, where it was analyzed the sensitivity for the NSI, using the full three neutrino probability in matter, assuming that the test values of the standard neutrino oscillation and for the test the NSI probability. It was made the marginalization over the parameters Δm_{31}^2 , θ_{23} , δ_{CP} and the complex phase of $\phi_{e\tau}$. We superimposed these sensitivity regions (shaded regions) in Figure 5. From this comparison, we have that

1. (i) the central region at 1σ can describe as the region where the θ_{23} of NSI probability is equal to the θ_{23} of standard probability. The point $(\epsilon_{ee}, \epsilon_{e\tau}) = (0, 0)$ correspond to the standard oscillation and for any value of ϵ_{ee} and $\epsilon_{e\tau}$ non-zero correspond to NSI probability that it is degenerated with the standard probability. This canceling of ϵ_{ee} and $\epsilon_{e\tau}$ effects it is similar to what was discussed in Section 5.1,
2. (ii) the external contours of the blue region can be understood as we can compensate for the large values of NSI by shifting the value of θ_{23} parameter, from the central value of the best-fit value to allowed at 3σ (shown by the dashed curves),
3. the anti-correlation of ϵ_{ee} and $\epsilon_{e\tau}$ can be understood by the analytical discussion made in Section 5.1 and also shown in Figure 4.

We can conclude that we can reasonably understand the behavior of the multiple solutions for the NSI parameters, from the sensitivity analysis of the DUNE experiment in Ref. [44], as the freedom to change the mixing angle θ_{23} and the combined phase ζ in such way that we have the same numerical value of the NSI probability and standard probability even for large NSI diagonal ϵ_{ee} ,

6 Conclusions

We study the effects of inclusion of NSI in the perturbative approach to neutrino oscillations in the matter through the Dyson Series. We developed a perturbative approach where the diagonal NSI parameters are kept non-perturbative and the NSI non-diagonal parameters

and the mixing parameters $\sin \theta_{13}$ and the ratio r_Δ as the perturbative parameters. We assume a hierarchy for NSI parameters, as $\tilde{\epsilon}_{e\tau}$ as sub-leading parameter and $\tilde{\epsilon}_{e\mu}$ and $\tilde{\epsilon}_{\mu\tau}$ as sub-sub-leading parameters. This choice has the advantage that we can get all other cases of perturbative expansions in the literature as case limits of our case, as we can appreciate in Table 2. Using this approach we compute as an example, the neutrino oscillation as given in Eq. (4.6) for the muon neutrino to electron neutrino conversion probability, and in Eq. (C.4) for the muon neutrino survival probability.

In Figure 1, we compare our analytical results (the black curve) with the numerical computation, shown in the dashed black line. The other results from perturbative approaches in the literature are also showed. For all choices of parameters, we are more trustworthy to the numerical computation than the other analytical perturbative computations available in the literature. Furthermore, as a by-product of our choice of NSI hierarchy is that the perturbed Hamiltonian in a block-diagonal format and this implies that we can describe the full probability as a function of $(\Lambda, \Gamma, \Sigma, \Omega)$ functions defined in Eq. (4.5).

Moreover, we have also have studied the underlying correlations between NSI parameters and mixing parameters that made there are multiple sets of NSI parameters and mixing angles that mostly have the same neutrino probability value. This degeneracy of the neutrino probability value that appears in numerical analysis in the literature, now it can be *explained* by the invariance of the amplitude and the phase of neutrino oscillation probability. This invariance was discussed in Section 5 for two cases, (i) involving only NSI parameters and (ii) involving a combination of the NSI parameters and the standard oscillation parameters. We discussed the necessary conditions to have the neutrino probability degeneracy, and we apply for these two cases. In Figure 2, we have shown the reason when we have multiple NSI, we can have a canceling effect and effectively get the same probability as is the probability without NSI. In Figure 5, we show in the plane of $\epsilon_{ee} \times \epsilon_{e\tau}$ where we made a numerical analysis of the sensitivity of a given experiment for NSI parameter, and it appears these two branches of solutions. It follows from our discussion in Section 5 the amplitude and the phase of $\epsilon_{e\tau}$ are kept unchanged even we change the value of mixing angle θ_{23} and the NSI parameters.

Finally, the fact that now we have oscillation formulas that can apply to most of the NSI allowed space of parameters should allow us to figure out the features of the future sets of experiments necessary to broken this degenerate behavior shown in the neutrino probabilities.

Acknowledgments

O.L.G.P. is grateful for the support of FAPESP funding Grant 2014/19164-6, CNPq research fellowship 306565/2019-6 and 304715/2016-6, and . O.L.G.P. and D.R.G. are grateful for partial support from the FAEPEX funding grant, No 2391/17. M. E. C. is grateful for the 140564/2018-7 and 130912/2016-6 funding from CNPQ. This study was financed in part by the Coordenação de Aperfeiçoamento de Pessoal de Nível Superior - Brasil

(CAPES) - Finance Code 001. The authors are thankful to M. C. Gonzalez-Garcia and M. Maltoni, who kindly share the table of the $\Delta\chi^2 \times \text{NSI}$ parameters.

References

- [1] SUPER-KAMIOKANDE collaboration, Y. Fukuda et al., *Evidence for oscillation of atmospheric neutrinos*, *Phys. Rev. Lett.* **81** (1998) 1562 [[hep-ex/9807003](#)].
- [2] GALLEX collaboration, P. Anselmann et al., *GALLEX results from the first 30 solar neutrino runs*, *Phys. Lett.* **B327** (1994) 377.
- [3] SAGE collaboration, P. Anselmann et al., *Results from SAGE (The Russian-American gallium solar neutrino experiment)*, *Physics Letters B* **328** (1994) 234 .
- [4] SUPER-KAMIOKANDE collaboration, S. Fukuda et al., *Constraints on neutrino oscillations using 1258 days of Super-Kamiokande solar neutrino data*, *Phys. Rev. Lett.* **86** (2001) 5656 [[hep-ex/0103033](#)].
- [5] SNO collaboration, Q. R. Ahmad et al., *Direct evidence for neutrino flavor transformation from neutral current interactions in the Sudbury Neutrino Observatory*, *Phys. Rev. Lett.* **89** (2002) 011301 [[nucl-ex/0204008](#)].
- [6] CHOOZ collaboration, M. Apollonio et al., *Search for neutrino oscillations on a long baseline at the CHOOZ nuclear power station*, *Eur. Phys. J.* **C27** (2003) 331 [[hep-ex/0301017](#)].
- [7] KAMLAND collaboration, K. Eguchi et al., *First results from KamLAND: Evidence for reactor anti-neutrino disappearance*, *Phys. Rev. Lett.* **90** (2003) 021802 [[hep-ex/0212021](#)].
- [8] DAYA BAY collaboration, F. P. An et al., *Observation of electron-antineutrino disappearance at Daya Bay*, *Phys. Rev. Lett.* **108** (2012) 171803 [[1203.1669](#)].
- [9] MINOS collaboration, P. Adamson et al., *Measurement of the Neutrino Mass Splitting and Flavor Mixing by MINOS*, *Phys. Rev. Lett.* **106** (2011) 181801 [[1103.0340](#)].
- [10] SOUDAN-2 collaboration, W. W. M. Allison et al., *The Atmospheric neutrino flavor ratio from a 3.9 fiducial kiloton year exposure of Soudan-2*, *Phys. Lett.* **B449** (1999) 137 [[hep-ex/9901024](#)].
- [11] MACRO collaboration, M. Ambrosio et al., *Measurement of the atmospheric neutrino induced upgoing muon flux using MACRO*, *Phys. Lett.* **B434** (1998) 451 [[hep-ex/9807005](#)].
- [12] ICECUBE collaboration, M. Aartsen et al., *Development of an analysis to probe the neutrino mass ordering with atmospheric neutrinos using three years of IceCube DeepCore data*, *Eur. Phys. J. C* **80** (2020) 9 [[1902.07771](#)].
- [13] T2K collaboration, K. Abe et al., *First measurement of the ν_μ charged-current cross section on a water target without pions in the final state*, *Phys. Rev.* **D97** (2018) 012001 [[1708.06771](#)].
- [14] T2K collaboration, K. Abe et al., *Constraint on the matter–antimatter symmetry-violating phase in neutrino oscillations*, *Nature* **580** (2020) 339.
- [15] I. Esteban, M. C. Gonzalez-Garcia, A. Hernandez-Cabezudo, M. Maltoni and T. Schwetz, *Global analysis of three-flavour neutrino oscillations: synergies and tensions in the determination of θ_{23} , δ_{CP} , and the mass ordering*, *JHEP* **01** (2019) 106 [[1811.05487](#)].

- [16] S. L. Glashow, J. Iliopoulos and L. Maiani, *Weak interactions with lepton-hadron symmetry*, *Phys. Rev. D* **2** (1970) 1285.
- [17] S. Weinberg, *A Model of Leptons*, *Phys. Rev. Lett.* **19** (1967) 1264.
- [18] A. Salam et al., *Elementary particle theory*, Ed. N. Svartholm, Stockholm, Almquist and Wiksell **367** (1968) 367.
- [19] F. Englert and R. Brout, *Broken Symmetry and the Mass of Gauge Vector Mesons*, *Phys. Rev. Lett.* **13** (1964) 321.
- [20] P. W. Higgs, *Broken symmetries, massless particles and gauge fields*, *Phys. Lett.* **12** (1964) 132.
- [21] P. W. Higgs, *Broken Symmetries and the Masses of Gauge Bosons*, *Phys. Rev. Lett.* **13** (1964) 508.
- [22] ATLAS collaboration, G. Aad et al., *Observation of a new particle in the search for the Standard Model Higgs boson with the ATLAS detector at the LHC*, *Phys. Lett. B* **716** (2012) 1 [1207.7214].
- [23] CMS collaboration, S. Chatrchyan et al., *Observation of a new boson at a mass of 125 GeV with the CMS experiment at the LHC*, *Phys. Lett. B* **716** (2012) 30 [1207.7235].
- [24] L. Wolfenstein, *Neutrino Oscillations in Matter*, *Phys. Rev. D* **17** (1978) 2369.
- [25] L. Wolfenstein, *Neutrino Oscillations and Stellar Collapse*, *Phys. Rev. D* **20** (1979) 2634.
- [26] M. M. Guzzo, A. Masiero and S. T. Petcov, *On the MSW effect with massless neutrinos and no mixing in the vacuum*, *Phys. Lett. B* **260** (1991) 154.
- [27] M. M. Guzzo and S. T. Petcov, *On the matter enhanced transitions of solar neutrinos in the absence of neutrino mixing in vacuum*, *Phys. Lett. B* **271** (1991) 172.
- [28] E. Roulet, *MSW effect with flavor changing neutrino interactions*, *Phys. Rev. D* **44** (1991) 935.
- [29] J. W. F. Valle, *Resonant oscillations of massless neutrinos in matter*, *Physics Letters B* **199** (1987) 432 .
- [30] K. Asano and H. Minakata, *Large- Θ_{13} Perturbation Theory of Neutrino Oscillation for Long-Baseline Experiments*, *JHEP* **06** (2011) 022 [1103.4387].
- [31] T. Ohlsson, *Status of non-standard neutrino interactions*, *Rept. Prog. Phys.* **76** (2013) 044201 [1209.2710].
- [32] O. G. Miranda and H. Nunokawa, *Non standard neutrino interactions: current status and future prospects*, *New J. Phys.* **17** (2015) 095002 [1505.06254].
- [33] I. Esteban, M. C. Gonzalez-Garcia and M. Maltoni, *On the Determination of Leptonic CP Violation and Neutrino Mass Ordering in Presence of Non-Standard Interactions: Present Status*, *JHEP* **06** (2019) 055 [1905.05203].
- [34] PARTICLE DATA GROUP collaboration, M. Tanabashi, K. Hagiwara, K. Hikasa, K. Nakamura, Y. Sumino, F. Takahashi et al., *Review of particle physics*, *Phys. Rev. D* **98** (2018) 030001.
- [35] Y. Grossman, *Nonstandard neutrino interactions and neutrino oscillation experiments*, *Phys. Lett. B* **359** (1995) 141 [hep-ph/9507344].

- [36] P. Krastev and J. N. Bahcall, *FCNC solutions to the solar neutrino problem*, in *Symposium on Flavor Changing Neutral Currents: Present and Future Studies (FCNC 97)*, pp. 259–263, 2, 1997, [hep-ph/9703267](#).
- [37] G. Brooijmans, *A Supersymmetric solution to the solar and atmospheric neutrino anomalies*, [hep-ph/9808498](#).
- [38] M. C. Gonzalez-Garcia, M. M. Guzzo, P. I. Krastev, H. Nunokawa, O. L. G. Peres, V. Pleitez et al., *Atmospheric neutrino observations and flavor changing interactions*, *Phys. Rev. Lett.* **82** (1999) 3202 [[hep-ph/9809531](#)].
- [39] S. Bergmann, M. M. Guzzo, P. de Holanda, P. Krastev and H. Nunokawa, *Status of the solution to the solar neutrino problem based on nonstandard neutrino interactions*, *Phys. Rev. D* **62** (2000) 073001 [[hep-ph/0004049](#)].
- [40] M. M. Guzzo, H. Nunokawa, P. C. de Holanda and O. L. G. Peres, *On the massless ‘just-so’ solution to the solar neutrino problem*, *Phys. Rev. D* **64** (2001) 097301 [[hep-ph/0012089](#)].
- [41] M. M. Guzzo, P. de Holanda, M. Maltoni, H. Nunokawa, M. Tortola and J. Valle, *Status of a hybrid three neutrino interpretation of neutrino data*, *Nucl. Phys. B* **629** (2002) 479 [[hep-ph/0112310](#)].
- [42] P. Coloma, A. Donini, J. Lopez-Pavon and H. Minakata, *Non-Standard Interactions at a Neutrino Factory: Correlations and CP violation*, *JHEP* **08** (2011) 036 [[1105.5936](#)].
- [43] A. De Gouvêa, K. J. Kelly, G. V. Stenico and P. Pasquini, *Physics with Beam Tau-Neutrino Appearance at DUNE*, *Phys. Rev. D* **100** (2019) 016004 [[1904.07265](#)].
- [44] P. Coloma and T. Schwetz, *Generalized mass ordering degeneracy in neutrino oscillation experiments*, *Phys. Rev. D* **94** (2016) 055005 [[1604.05772](#)].
- [45] P. Coloma, P. B. Denton, M. Gonzalez-Garcia, M. Maltoni and T. Schwetz, *Curtailing the Dark Side in Non-Standard Neutrino Interactions*, *JHEP* **04** (2017) 116 [[1701.04828](#)].
- [46] O. Yasuda, *Neutrino Oscillations at low energy long baseline experiments in the presence of nonstandard interactions and parameter degeneracy*, *PTEP* **2020** (2020) 063B03 [[2002.01616](#)].
- [47] Z. Rahman, A. Dasgupta and R. Adhikari, *The Discovery reach of CP violation in neutrino oscillation with non-standard interaction effects*, *J. Phys. G* **42** (2015) 065001 [[1503.03248](#)].
- [48] I. Girardi, D. Meloni and S. Petcov, *The Daya Bay and T2K results on $\sin^2 2\theta_{13}$ and Non-Standard Neutrino Interactions*, *Nucl. Phys. B* **886** (2014) 31 [[1405.0416](#)].
- [49] R. Szafron and M. Zralek, *Oscillation of Dirac and Majorana neutrinos from muon decay in the case of a general interaction*, *Phys. Lett. B* **718** (2012) 113 [[1210.2996](#)].
- [50] B. Dutta, R. F. Lang, S. Liao, S. Sinha, L. Strigari and A. Thompson, *A global analysis strategy to resolve neutrino NSI degeneracies with scattering and oscillation data*, [2002.03066](#).
- [51] S. Choubey and D. Pramanik, *On Resolving the Dark LMA Solution at Neutrino Oscillation Experiments*, [1912.08629](#).
- [52] Y. Farzan and M. Tortola, *Neutrino oscillations and Non-Standard Interactions*, *Front. in Phys.* **6** (2018) 10 [[1710.09360](#)].
- [53] J. Liao, D. Marfatia and K. Whisnant, *Nonstandard neutrino interactions at DUNE, T2HK and T2HKK*, *JHEP* **01** (2017) 071 [[1612.01443](#)].

- [54] J. Tang and Y. Zhang, *Study of nonstandard charged-current interactions at the MOMENT experiment*, *Phys. Rev. D* **97** (2018) 035018 [[1705.09500](#)].
- [55] K. Babu, D. Gonçalves, S. Jana and P. A. Machado, *Neutrino Non-Standard Interactions: Complementarity Between LHC and Oscillation Experiments*, [2003.03383](#).
- [56] K. Babu, G. Chauhan and P. Bhupal Dev, *Neutrino Non-Standard Interactions via Light Scalars in the Earth, Sun, Supernovae and the Early Universe*, *Phys. Rev. D* **101** (2020) 095029 [[1912.13488](#)].
- [57] S. Demidov, *Bounds on non-standard interactions of neutrinos from IceCube DeepCore data*, *JHEP* **03** (2020) 105 [[1912.04149](#)].
- [58] F. Capozzi, S. S. Chatterjee and A. Palazzo, *Neutrino Mass Ordering Obscured by Nonstandard Interactions*, *Phys. Rev. Lett.* **124** (2020) 111801 [[1908.06992](#)].
- [59] W.-J. Feng, J. Tang, T.-C. Wang and Y.-X. Zhou, *Nonstandard interactions versus planet-scale neutrino oscillations*, *Phys. Rev. D* **100** (2019) 115034 [[1909.12674](#)].
- [60] SUPER-KAMIOKANDE collaboration, G. Mitsuka et al., *Study of Non-Standard Neutrino Interactions with Atmospheric Neutrino Data in Super-Kamiokande I and II*, *Phys. Rev. D* **84** (2011) 113008 [[1109.1889](#)].
- [61] W. Altmannshofer, M. Tammara and J. Zupan, *Non-standard neutrino interactions and low energy experiments*, *JHEP* **09** (2019) 083 [[1812.02778](#)].
- [62] P. Coloma, *Non-Standard Interactions in propagation at the Deep Underground Neutrino Experiment*, *JHEP* **03** (2016) 016 [[1511.06357](#)].
- [63] T. Ohlsson, H. Zhang and S. Zhou, *Probing the leptonic Dirac CP-violating phase in neutrino oscillation experiments*, *Phys. Rev. D* **87** (2013) 053006 [[1301.4333](#)].
- [64] S. Choubey, A. Ghosh, T. Ohlsson and D. Tiwari, *Neutrino Physics with Non-Standard Interactions at INO*, *JHEP* **12** (2015) 126 [[1507.02211](#)].
- [65] S.-F. Ge and A. Yu. Smirnov, *Non-standard interactions and the CP phase measurements in neutrino oscillations at low energies*, *JHEP* **10** (2016) 138 [[1607.08513](#)].
- [66] G. Barenboim, C. A. Ternes and M. Tórtola, *New physics vs new paradigms: distinguishing CPT violation from NSI*, *Eur. Phys. J. C* **79** (2019) 390 [[1804.05842](#)].
- [67] S. Pandey, S. Karmakar and S. Rakshit, *Strong constraints on non-standard neutrino interactions: LHC vs. IceCube*, *JHEP* **11** (2019) 046 [[1907.07700](#)].
- [68] A. de Gouvêa and K. J. Kelly, *Non-standard Neutrino Interactions at DUNE*, *Nucl. Phys. B* **908** (2016) 318 [[1511.05562](#)].
- [69] L. J. Flores, E. A. Garcés and O. G. Miranda, *Exploring NSI degeneracies in long-baseline experiments*, *Phys. Rev. D* **98** (2018) 035030 [[1806.07951](#)].
- [70] A. Falkowski, G. Grilli di Cortona and Z. Tabrizi, *Future DUNE constraints on EFT*, *JHEP* **04** (2018) 101 [[1802.08296](#)].
- [71] A. Chatterjee, F. Kamiya, C. A. Moura and J. Yu, *Impact of Matter Density Profile Shape on Non-Standard Interactions at DUNE*, [1809.09313](#).
- [72] I. Bischer and W. Rodejohann, *General Neutrino Interactions at the DUNE Near Detector*, *Phys. Rev. D* **99** (2019) 036006 [[1810.02220](#)].

- [73] T. Kikuchi, H. Minakata and S. Uchinami, *Perturbation Theory of Neutrino Oscillation with Nonstandard Neutrino Interactions*, *JHEP* **03** (2009) 114 [[0809.3312](#)].
- [74] J. Liao, D. Marfatia and K. Whisnant, *Degeneracies in long-baseline neutrino experiments from nonstandard interactions*, *Phys. Rev.* **D93** (2016) 093016 [[1601.00927](#)].
- [75] K. N. Deepthi, S. Goswami and N. Nath, *Can nonstandard interactions jeopardize the hierarchy sensitivity of DUNE?*, *Phys. Rev.* **D96** (2017) 075023 [[1612.00784](#)].
- [76] K. N. Deepthi, S. Goswami and N. Nath, *Challenges posed by non-standard neutrino interactions in the determination of δ_{CP} at DUNE*, *Nucl. Phys.* **B936** (2018) 91 [[1711.04840](#)].
- [77] U. K. Dey, N. Nath and S. Sadhukhan, *Non-Standard Neutrino Interactions in a Modified $\nu 2HDM$* , *Phys. Rev.* **D98** (2018) 055004 [[1804.05808](#)].
- [78] O. Yasuda, *On the exact formula for neutrino oscillation probability by Kimura, Takamura and Yokomakura*, [0704.1531](#).
- [79] D. Meloni, T. Ohlsson and H. Zhang, *Exact and Approximate Formulas for Neutrino Mixing and Oscillations with Non-Standard Interactions*, *JHEP* **04** (2009) 033 [[0901.1784](#)].
- [80] D. Meloni, T. Ohlsson, W. Winter and H. Zhang, *Non-standard interactions versus non-unitary lepton flavor mixing at a neutrino factory*, *JHEP* **04** (2010) 041 [[0912.2735](#)].
- [81] J. Kopp, M. Lindner, T. Ota and J. Sato, *Non-standard neutrino interactions in reactor and superbeam experiments*, *Phys. Rev.* **D77** (2008) 013007 [[0708.0152](#)].
- [82] M. Blennow, S. Choubey, T. Ohlsson, D. Pramanik and S. K. Raut, *A combined study of source, detector and matter non-standard neutrino interactions at DUNE*, *JHEP* **08** (2016) 090 [[1606.08851](#)].
- [83] A. Chatterjee, P. Mehta, D. Choudhury and R. Gandhi, *Testing nonstandard neutrino matter interactions in atmospheric neutrino propagation*, *Phys. Rev.* **D93** (2016) 093017 [[1409.8472](#)].
- [84] M. Masud, A. Chatterjee and P. Mehta, *Probing CP violation signal at DUNE in presence of non-standard neutrino interactions*, *J. Phys.* **G43** (2016) 095005 [[1510.08261](#)].
- [85] M. Masud and P. Mehta, *Nonstandard interactions spoiling the CP violation sensitivity at DUNE and other long baseline experiments*, *Phys. Rev.* **D94** (2016) 013014 [[1603.01380](#)].
- [86] M. Masud and P. Mehta, *Nonstandard interactions and resolving the ordering of neutrino masses at DUNE and other long baseline experiments*, *Phys. Rev.* **D94** (2016) 053007 [[1606.05662](#)].
- [87] M. Masud, S. Roy and P. Mehta, *Correlations and degeneracies among the NSI parameters with tunable beams at DUNE*, *Phys. Rev.* **D99** (2019) 115032 [[1812.10290](#)].
- [88] M. M. Guzzo, P. C. de Holanda and O. L. G. Peres, *Effects of nonstandard neutrino interactions on MSW - LMA solution to the solar neutrino problems*, *Phys. Lett. B* **591** (2004) 1 [[hep-ph/0403134](#)].
- [89] O. G. Miranda, M. A. Tortola and J. W. F. Valle, *Are solar neutrino oscillations robust?*, *JHEP* **10** (2006) 008 [[hep-ph/0406280](#)].
- [90] A. Friedland, C. Lunardini and M. Maltoni, *Atmospheric neutrinos as probes of neutrino-matter interactions*, *Phys. Rev.* **D70** (2004) 111301 [[hep-ph/0408264](#)].

- [91] I. Esteban, M. C. Gonzalez-Garcia, M. Maltoni, I. Martinez-Soler and J. Salvado, *Updated Constraints on Non-Standard Interactions from Global Analysis of Oscillation Data*, *JHEP* **08** (2018) 180 [[1805.04530](#)].
- [92] J. Barranco, O. Miranda and T. Rashba, *Probing new physics with coherent neutrino scattering off nuclei*, *JHEP* **12** (2005) 021 [[hep-ph/0508299](#)].
- [93] PARTICLE DATA GROUP collaboration, M. Tanabashi et al., *Review of Particle Physics*, *Phys. Rev. D* **98** (2018) 030001.
- [94] COHERENT collaboration, D. Akimov et al., *Observation of Coherent Elastic Neutrino-Nucleus Scattering*, *Science* **357** (2017) 1123 [[1708.01294](#)].
- [95] CONNIE collaboration, A. Aguilar-Arevalo et al., *Exploring low-energy neutrino physics with the Coherent Neutrino Nucleus Interaction Experiment*, *Phys. Rev. D* **100** (2019) 092005 [[1906.02200](#)].
- [96] CONNIE collaboration, A. Aguilar-Arevalo et al., *Search for light mediators in the low-energy data of the CONNIE reactor neutrino experiment*, *JHEP* **04** (2020) 054 [[1910.04951](#)].
- [97] J. Liao and D. Marfatia, *COHERENT constraints on nonstandard neutrino interactions*, *Phys. Lett. B* **775** (2017) 54 [[1708.04255](#)].
- [98] I. M. Shoemaker, *COHERENT search strategy for beyond standard model neutrino interactions*, *Phys. Rev. D* **95** (2017) 115028 [[1703.05774](#)].
- [99] M. C. Gonzalez-Garcia, M. Maltoni, Y. F. Perez-Gonzalez and R. Zukanovich Funchal, *Neutrino Discovery Limit of Dark Matter Direct Detection Experiments in the Presence of Non-Standard Interactions*, *JHEP* **07** (2018) 019 [[1803.03650](#)].
- [100] Y. Farzan, M. Lindner, W. Rodejohann and X.-J. Xu, *Probing neutrino coupling to a light scalar with coherent neutrino scattering*, *JHEP* **05** (2018) 066 [[1802.05171](#)].
- [101] P. B. Denton, Y. Farzan and I. M. Shoemaker, *Testing large non-standard neutrino interactions with arbitrary mediator mass after COHERENT data*, *JHEP* **07** (2018) 037 [[1804.03660](#)].
- [102] D. Aristizabal Sierra, V. De Romeri and N. Rojas, *COHERENT analysis of neutrino generalized interactions*, *Phys. Rev. D* **98** (2018) 075018 [[1806.07424](#)].
- [103] P. Coloma, I. Esteban, M. Gonzalez-Garcia and M. Maltoni, *Improved global fit to Non-Standard neutrino Interactions using COHERENT energy and timing data*, *JHEP* **02** (2020) 023 [[1911.09109](#)].
- [104] C. Giunti, *General COHERENT constraints on neutrino nonstandard interactions*, *Phys. Rev. D* **101** (2020) 035039 [[1909.00466](#)].
- [105] B. Canas, E. Garces, O. Miranda, A. Parada and G. Sanchez Garcia, *Interplay between nonstandard and nuclear constraints in coherent elastic neutrino-nucleus scattering experiments*, *Phys. Rev. D* **101** (2020) 035012 [[1911.09831](#)].
- [106] M. C. Gonzalez-Garcia and M. Maltoni, *Table of the $\Delta\chi^2 \times$ NSI parameters for the analysis made in Ref.[103]*.
- [107] A. Cervera, A. Donini, M. B. Gavela, J. J. Gomez Cadenas, P. Hernandez, O. Mena et al., *Golden measurements at a neutrino factory*, *Nucl. Phys. B* **579** (2000) 17 [[hep-ph/0002108](#)].

- [108] E. K. Akhmedov, R. Johansson, M. Lindner, T. Ohlsson and T. Schwetz, *Series expansions for three flavor neutrino oscillation probabilities in matter*, *JHEP* **04** (2004) 078 [[hep-ph/0402175](#)].
- [109] E. K. Akhmedov, P. Huber, M. Lindner and T. Ohlsson, *T violation in neutrino oscillations in matter*, *Nucl. Phys.* **B608** (2001) 394 [[hep-ph/0105029](#)].
- [110] C. Giunti and C. W. Kim, *Fundamentals of Neutrino Physics and Astrophysics*. Oxford, UK: Univ. Pr. (2007) 710 p, 2007.
- [111] K. Kimura, A. Takamura and H. Yokomakura, *Exact formula of probability and CP violation for neutrino oscillations in matter*, *Phys. Lett.* **B537** (2002) 86 [[hep-ph/0203099](#)].
- [112] T. Ohlsson and H. Snellman, *Three flavor neutrino oscillations in matter*, *J. Math. Phys.* **41** (2000) 2768 [[hep-ph/9910546](#)].
- [113] J. J. Sakurai and E. D. Commins, *Modern quantum mechanics, revised edition*, 1995.
- [114] H. W. Zaglauer and K. H. Schwarzer, *The Mixing Angles in Matter for Three Generations of Neutrinos and the MSW Mechanism*, *Z. Phys.* **C40** (1988) 273.
- [115] J. Bellandi, M. M. Guzzo and V. Aquino, *On Resonances and Mixing Angles in Three Neutrino Oscillations in Matter*, *Brazilian Journal of Physics* **27** (1997) .
- [116] P. B. Denton, H. Minakata and S. J. Parke, *Compact Perturbative Expressions For Neutrino Oscillations in Matter*, *JHEP* **06** (2016) 051 [[1604.08167](#)].
- [117] A. Ioannisian and S. Pokorski, *Three Neutrino Oscillations in Matter*, *Phys. Lett.* **B782** (2018) 641 [[1801.10488](#)].
- [118] RENO collaboration, J. K. Ahn et al., *Observation of Reactor Electron Antineutrino Disappearance in the RENO Experiment*, *Phys. Rev. Lett.* **108** (2012) 191802 [[1204.0626](#)].
- [119] H. Minakata and S. J. Parke, *Simple and Compact Expressions for Neutrino Oscillation Probabilities in Matter*, *JHEP* **01** (2016) 180 [[1505.01826](#)].
- [120] DUNE collaboration, B. Abi et al., *The DUNE Far Detector Interim Design Report Volume 1: Physics, Technology and Strategies*, [1807.10334](#).
- [121] Numpy and S. Documentation. <https://docs.scipy.org/doc/>.
- [122] K. Kimura, A. Takamura and H. Yokomakura, *Exact formulas and simple CP dependence of neutrino oscillation probabilities in matter with constant density*, *Phys. Rev.* **D66** (2002) 073005 [[hep-ph/0205295](#)].
- [123] I. Esteban, M. C. Gonzalez-Garcia, M. Maltoni, I. Martinez-Soler and T. Schwetz, *Updated fit to three neutrino mixing: exploring the accelerator-reactor complementarity*, *JHEP* **01** (2017) 087 [[1611.01514](#)].
- [124] M. E. Chaves, *Métodos analíticos para a evolução de neutrinos na matéria sob a influência de interações não-padrão*, Master's thesis, Universidade Federal Fluminense, RJ, Brazil, 2018. In portuguese, <https://app.uff.br/riuff/handle/1/7439>.

A Explicit relation between NSI parameters in flavor basis and propagation basis

The rotation which relates flavor and propagation basis from Eq. (3.2) and with the redefinition given in Eq. (1.7) implies in the following relation between NSI parameters:

$$\begin{aligned}
\tilde{\epsilon}_{\mu\mu} &= s_{23}^2 \epsilon_{\tau\tau} - 2c_{23}s_{23}\Re(\epsilon_{\mu\tau}) \\
\tilde{\epsilon}_{\tau\tau} &= c_{23}^2 \epsilon_{\tau\tau} + 2c_{23}s_{23}\Re(\epsilon_{\mu\tau}) \\
\tilde{\epsilon}_{\mu\tau} &= -s_{23}c_{23}\epsilon_{\tau\tau} + (c_{23}^2 - s_{23}^2)\Re(\epsilon_{\mu\tau}) + i\Im(\epsilon_{\mu\tau}) \\
\tilde{\epsilon}_{ee} &= \epsilon_{ee} \\
\tilde{\epsilon}_{e\mu} &= c_{23}\epsilon_{e\mu} - s_{23}\epsilon_{e\tau} \\
\tilde{\epsilon}_{e\tau} &= s_{23}\epsilon_{e\mu} + c_{23}\epsilon_{e\tau}
\end{aligned} \tag{A.1}$$

B Formalism to perturbation theory for neutrino oscillations

The S matrix is responsible for the neutrino-state time evolution,

$$|\nu_\beta(t)\rangle = S_{\beta\alpha}(t)|\nu_\alpha(0)\rangle, \tag{B.1}$$

where the operator $S(t)$ is given by,

$$S(t) = \mathcal{T} \exp \left\{ -i \int_0^t H(t') dt' \right\}. \tag{B.2}$$

Here \mathcal{T} means temporal ordering. The oscillation probability follows from

$$P(\nu_\alpha \rightarrow \nu_\beta) \equiv P_{\nu_\alpha \rightarrow \nu_\beta} = |S_{\beta\alpha}|^2. \tag{B.3}$$

From Eq. (3.9) we define the potential $\tilde{V} = \tilde{H} - \tilde{H}^{(0)}$, which in the interaction picture assumes the form,

$$\tilde{V}_I = e^{i\tilde{H}^{(0)}t} \tilde{V} e^{-i\tilde{H}^{(0)}t}, \tag{B.4}$$

where \tilde{V} is the time-dependent potential in the Schrodinger picture. The time-evolution operator in the interaction picture can be defined as [113] $\Omega(x)$,

$$\Omega(t) = e^{i\tilde{H}^{(0)}t} \tilde{S}(t), \tag{B.5}$$

which must obey the operator time evolution equation:

$$i \frac{d}{dt} \Omega(t) = \tilde{V}_I \Omega(t), \tag{B.6}$$

which is subjected to the initial condition $\Omega(t=0)1$. The Eq. (B.6) plus the initial condition implies in the integral equation:

$$\Omega(t) = 1 - i \int_0^t \tilde{V}_I(t') \Omega(t') dt'. \tag{B.7}$$

The recursive substitution of $\Omega(x)$ into Eq. (B.7) leads to the Dyson Series, which gives the solution for Eq. (B.6) as:

$$\begin{aligned}\Omega(x) = & 1 + (-i) \int_0^x \tilde{V}_I(x') dx' + (-i)^2 \int_0^x \tilde{V}_I(x') dx' \int_0^{x'} \tilde{V}_I(x'') dx'' \\ & + (-i)^3 \int_0^x \tilde{V}_I(x') dx' \int_0^{x'} \tilde{V}_I(x'') dx'' \int_0^{x''} \tilde{V}_I(x''') dx''' + \mathcal{O}(\epsilon^2).\end{aligned}\quad (\text{B.8})$$

Once $\Omega(x)$ is determinate from Eq. (B.8), in the propagation basis

$$\tilde{S}(x) = e^{-i\tilde{H}^{(0)}} \Omega(x). \quad (\text{B.9})$$

The S matrix can then be written in the flavor basis as

$$S = [\mathbf{R}(\theta_{23})]^\dagger \tilde{S} \mathbf{R}(\theta_{23}). \quad (\text{B.10})$$

The \tilde{S} matrix is explicitly calculated in [124].

C Muon neutrino survival probability

Here we show our results for muon neutrino survival probability obtained from the same procedure explained in Section 3. We consider terms until $n \leq 3/2$. The resulting formulas show the same functional structure of standard oscillation formalism, and the NSI features are incorporated in the $(\Sigma, \Omega, \Lambda, \Gamma)$ quantities,

$$P_{\nu_\mu \nu_\mu}^{(0)} = 1 - 4c_{23}^2 s_{23}^2 \sin^2 \left(\frac{\Delta_{31} x r_A \Lambda}{2} \right), \quad (\text{C.1})$$

$$\begin{aligned}P_{\nu_\mu \nu_\mu}^{(1)} = & -\frac{4|\Sigma|^2 s_{23}^4}{r_A^2 (\Gamma - \Lambda)^2} \sin^2 \left(\frac{\Delta_{31} x r_A (\Gamma - \Lambda)}{2} \right) \\ & + 2c_{23}^2 s_{23}^2 \left(c_{12}^2 r_A + \frac{|\Sigma|^2}{r_A (\Gamma - \Lambda)} + s_{13}^2 \right) \sin(\Delta_{31} x r_A \Lambda) (\Delta_{31} x) \\ & + \frac{2|\Sigma|^2 s_{23}^2 c_{23}^2}{r_A^2 (\Gamma - \Lambda)^2} [\cos(\Delta_{31} x r_A \Gamma) - \cos(\Delta_{31} x r_A \Lambda)] \\ & - \frac{8|\tilde{\epsilon}_{\mu\tau}| c_{23} s_{23} (c_{23}^2 - s_{23}^2) \cos(\tilde{\phi}_{\mu\tau})}{\Lambda} \sin^2 \left(\frac{\Delta_{31} x \Lambda r_A}{2} \right),\end{aligned}\quad (\text{C.2})$$

$$\begin{aligned}P_{\nu_\mu \nu_\mu}^{(3/2)} = & -\frac{8r_A c_{12} s_{12} c_{23} s_{23} s_{13} (c_{23}^2 - s_{23}^2) \cos(\delta_{\text{CP}})}{r_A \Lambda} \sin^2 \left(\frac{\Delta_{31} x r_A \Lambda}{2} \right) \\ & + \frac{4|\Omega\Sigma| c_{23} s_{23} \cos(\phi_\Sigma - \phi_\Omega)}{r_A^2 \Gamma (\Gamma - \Lambda)} (c_{23}^2 \cos(\Delta_{31} x r_A \Gamma) - c_{23}^2 + s_{23}^2) \cos(\Delta_{31} x r_A (\Gamma - \Lambda)) \\ & - \frac{4|\Omega\Sigma| c_{23} s_{23} \cos(\phi_\Sigma - \phi_\Omega)}{\Lambda r_A^2 (\Gamma - \Lambda)} (c_{23}^2 \cos(\Delta_{31} x r_A \Lambda) + 1) \\ & + \frac{4|\Omega\Sigma| c_{23} s_{23} \cos(\phi_\Sigma - \phi_\Omega)}{r_A^2 \Gamma \Lambda} (s_{23}^2 \cos \Delta_{31} x r_A \Lambda).\end{aligned}\quad (\text{C.3})$$

The muon neutrino probability it is

$$P^{\text{perturbative}}(\nu_\mu \nu_\mu) = P(\nu_\mu \nu_\mu)^{(0)} + P(\nu_\mu \nu_\mu)^{(1)} + P(\nu_\mu \nu_\mu)^{(3/2)}. \quad (\text{C.4})$$

D The Non-Standard Interaction Degeneracy

We will discuss the conditions to have the standard oscillation probability to exactly degenerate with NSI oscillation probability.

Here, from Eq. (5.24), we will derive Eq. (5.25). Substituting the explicit expression for the probability, Eq. (4.2), on the expression for the degeneracy condition, Eq. (5.24), it give us

$$\begin{aligned} \left[P^{(1)}(\nu_\mu \rightarrow \nu_e)(\tilde{\epsilon}_{\alpha\beta}, \boldsymbol{\theta}_{23}) \right]^{(\text{NSI})} &= \left[P^{(1)}(\nu_\mu \rightarrow \nu_e)(\tilde{\epsilon}_{\alpha\beta} = 0, \theta_{23}) \right]^{(\text{SO})} \\ 4 \frac{|\Sigma|^2 (\boldsymbol{s}_{23})^2}{r_A^2 \eta^2} \sin^2 \left(\frac{\Delta_{31} x}{2} r_A \eta \right) &= 4 \frac{s_{13}^2 s_{23}^2}{(1 - r_A)^2} \sin^2 \left(\frac{\Delta_{31} x}{2} (1 - r_A) \right), \end{aligned} \quad (\text{D.1})$$

that can be written as

$$\frac{r_A^2}{s_{13}^2} |\tilde{\epsilon}_{e\tau}|^2 + 2 \frac{r_A}{s_{13}} |\tilde{\epsilon}_{e\tau}| \cos(\zeta) + 1 = \left(\frac{s_{23}}{\boldsymbol{s}_{23}} \right)^2 \frac{\text{sinc}^2(\Delta_{31} x (1 - r_A))}{\text{sinc}^2(\Delta_{31} x \eta)}, \quad (\text{D.2})$$

where the functions $\text{sinc}(x)$ are defined as $\text{sinc}(x) \equiv \frac{\sin(x)}{x}$. We can expand the $\text{sinc}(\Delta_{31} x \eta)$ around the standard oscillation phase, and it will give us

$$\frac{\text{sinc}^2(\Delta_{31} x (1 - r_A))}{\text{sinc}^2(\Delta_{31} x \eta)} \approx \left(\frac{\text{sinc}(\Delta_{31} x (1 - r_A))}{\text{sinc}(\Delta_{31} x (1 - r_A)) + B_2 r_A (\tilde{\epsilon}_{ee} - \tilde{\epsilon}_{\tau\tau})} \right)^2, \quad (\text{D.3})$$

where can define the quantities

$$\begin{aligned} B_1 &= \text{sinc} \left(\frac{\Delta_{31} x}{2} (1 - r_A) \right), \\ B_2 &= \left(\frac{\Delta_{31} x}{2} \right) \frac{\cos \left(\frac{\Delta_{31} x}{2} (1 - r_A) \right) - \text{sinc} \left(\frac{\Delta_{31} x}{2} (1 - r_A) \right)}{\left(\frac{\Delta_{31} x}{2} (1 - r_A) \right)}. \end{aligned} \quad (\text{D.4})$$

Replacing Eq. (D.3) into Eq. (D.2) we have

$$\frac{r_A^2}{s_{13}^2} |\tilde{\epsilon}_{e\tau}|^2 + 2 \frac{r_A}{s_{13}} |\tilde{\epsilon}_{e\tau}| \cos(\zeta) + 1 = \left(\frac{s_{23}}{\boldsymbol{s}_{23}} \right)^2 \left(\frac{B_1}{B_1 + B_2 r_A (\tilde{\epsilon}_{ee} - \tilde{\epsilon}_{\tau\tau})} \right)^2. \quad (\text{D.5})$$

where this relation give the condition for the equality of neutrino probabilities for a given set of NSI parameters $\tilde{\epsilon}_{ee}, \tilde{\epsilon}_{\tau\tau}, \tilde{\epsilon}_{e\tau}$, (ζ and the mixing angle θ_{23}).